

Chapter 2

Magnetohydrodynamics of the Cosmic Plasma

2.1 Hydrodynamic Equations of the Neutral Gas

Table 1.1 shows that the cosmic media can have very different properties as their parameters vary within exceptionally broad ranges. In particular, the gas ionization can vary from almost zero (neutral media, e.g., clouds of cold neutral hydrogen) to almost unity (fully ionized plasma). It is worthwhile, therefore, to start with a simpler case of equation set for the neutral gas. We assume that the reader is familiar with the hydrodynamics (HD) fundamentals, so we just remind the equations and briefly discuss the meaning of the terms entering them without going into the detail too deeply. The relation of HD to the kinetic theory has been outlined in Sect. 1.3.

Two basic HD equations (see Sect. 1.3.3) are the continuity equation

$$\frac{\partial \rho}{\partial t} + \nabla \cdot \rho \mathbf{u} = 0 \quad (2.1)$$

and equation of motion

$$\rho \left(\frac{\partial \mathbf{u}}{\partial t} + (\mathbf{u} \cdot \nabla) \mathbf{u} \right) = -\nabla p + \mathbf{f} + \eta \Delta \mathbf{u} + \frac{\eta}{3} \nabla (\nabla \cdot \mathbf{u}), \quad (2.2)$$

where $\rho(\mathbf{r}, t)$ is the *mass density*, $\mathbf{u}(\mathbf{r}, t)$ is the macroscopic *velocity*, \mathbf{f} is the *volume force* applied to the medium (e.g., gravitation force), and p is the gas pressure. Everywhere below we will consider “simple” media, which can be correctly described by a single viscosity coefficient, η . In case of “complex” media composed of the particles with essential role of the internal degrees of freedom, e.g., dust particles, a so-called second viscosity (Landau and Lifshitz 1966) may come into play; very few papers consider this effect in the astrophysics context, so we entirely neglect the second viscosity in this book. If the usual (first) viscosity is also neglected, Eq. (2.2) reduces to **Euler**

equation (2.7b); see below. If the liquid is incompressible, $\rho = \text{const}$, and so $\nabla \cdot \mathbf{u} = 0$, then the last term in Eq. (2.2) drops out from the equation and it reduces to the **Navier–Stokes equation**. These equations must be complemented by the equation of state

$$p = p(\rho, s), \quad (2.3)$$

where s is the **specific entropy** (entropy per unit mass); hereafter we call it **entropy** for brevity.

When energy dissipation occurs in the gas studied, the entropy increases, which is described by the equation

$$\rho T \left(\frac{\partial s}{\partial t} + (\mathbf{u} \cdot \nabla) s \right) = \Pi_{\alpha\beta} \nabla_\beta u_\alpha + \nabla \cdot (\chi \nabla T), \quad (2.4)$$

where

$$\Pi_{\alpha\beta} = \eta \left(\frac{\partial u_\alpha}{\partial x_\beta} + \frac{\partial u_\beta}{\partial x_\alpha} - \frac{2}{3} (\nabla \cdot \mathbf{u}) \delta_{\alpha\beta} \right) \quad (2.5)$$

is the **tensor of viscous tensions** [cf. Eq. (1.72)] and T is the **temperature** in energy units. The specific entropy s has the dimension of reverse mass; thus, the full entropy of the entire physical system $S = \int \rho s \, dV$ is dimensionless. If the temperature is measured in Kelvin [K], the full entropy must be multiplied by Boltzmann constant $k_B \approx 1.38 \times 10^{-23} \text{ J/K} \approx 1.38 \times 10^{-16} \text{ erg/K}$. Here the coefficient of the **dynamic viscosity** η and coefficient of the **heat conductivity** χ are assumed to be known. In principle, these coefficients can be calculated within the physics kinetics; see Sect. 1.3.7, where these coefficients are estimated for a collisional plasma.

For closure of equation set (2.1)–(2.5) we must either express the temperature $T(\rho, s)$ via the density and the entropy or express the entropy $s(\rho, T)$ via the density and the temperature by using thermodynamic relations and the equation of state, then the number of equations becomes equal to the number of unknowns. In practice, however, the thermodynamic relations are unknown for an arbitrary medium. Nevertheless, for the tenuous gas considered here, the approximation of rarefied (“ideal”) gas is sufficient for most of the practical applications.

2.1.1 General Properties

Let us discuss some global properties of the HD equations. Set of equations (2.1)–(2.5) is nonlinear in a general case and so very complicated. To obtain an analytical solution of the equations requires some simplifying assumptions and approximations to be made. One of the approximations frequently used in the astrophysical studies is the approximation of *ideal HD*, when the dissipative processes can be discarded. The applicability of this approximation

is not guaranteed and so must be justified in each given case. A necessary condition for the ideal HD to work is the inequality

$$R = \frac{ul}{\nu} \gg 1, \quad (2.6)$$

where u is the typical velocity value, l is the characteristic scale of the velocity variation, and $\nu \equiv \eta/\rho$ is the kinematic viscosity. The dimensionless parameter R is called the **Reynolds number**; it plays a very important role in HD.

If inequality (2.6) is fulfilled and the temperature gradient is small or evanescent, then we can completely neglect the dissipative terms in Eqs. (2.1)–(2.5). Apparently, the entropy is constant in this case, while the set of HD equations simplifies to the form:

$$\frac{\partial \rho}{\partial t} + \nabla(\rho \mathbf{u}) = 0, \quad (2.7a)$$

$$\frac{\partial \mathbf{u}}{\partial t} + (\mathbf{u} \cdot \nabla) \mathbf{u} = -\frac{1}{\rho} \nabla p + \frac{1}{\rho} \mathbf{f}, \quad (2.7b)$$

$$\frac{ds}{dt} \equiv \frac{\partial s}{\partial t} + (\mathbf{u} \cdot \nabla) s = 0, \quad p = p(\tau, s). \quad (2.7c)$$

Equation (2.7c) for the entropy describes its constancy in every moving macroscopic element of the medium; the derivative $d/dt = \partial/\partial t + (\mathbf{u} \cdot \nabla)$ is called the **material derivative**. If the medium is uniform in the beginning, Eq. (2.7c) can be replaced by the condition of the global constancy of the entropy:

$$s = \text{const.} \quad (2.8)$$

It is worthwhile to keep in mind that the HD (or, more appropriately, the *gas dynamics*, *GD*)¹ can only be applied to the substances in the state of the *local thermodynamic equilibrium*. Stated another way, this means that one can define small macroscopic volume elements (with a linear scale l) in each of which the particles have *equilibrium* (e.g., *Maxwellian*) distribution with almost constant density, velocity, and temperature within each element. The gradients of these measures as well as their time variations must be small, i.e., the following inequalities must hold:

$$\left| \frac{\Lambda}{f} \frac{\partial f}{\partial x} \right| \ll 1, \quad \left| \frac{\tau}{f} \frac{\partial f}{\partial t} \right| \ll 1, \quad \text{or} \quad l \gg \Lambda, \quad \Delta t \gg \tau, \quad (2.9)$$

where f is any of the ρ , T , and \mathbf{u} values; Λ is the mean free path of the particles between collisions; τ is the mean time between the collisions; and Δt and l are the macroscopically small intervals. Even with these simplifications, the HD equations remain nonlinear and, thus, highly sophisticated.

¹The term GD is more appropriate in our case because the astrophysical media represent typically a gas (neutral or ionized) phase rather than a fluid, which would imply use of the term “hydro” (water).

2.2 MHD Equations

The phenomena in the gas phase and the set of equations describing them are even more complicated if the medium possesses electric conductivity σ and contains the magnetic field \mathbf{B} . The magnetic field can be generated by both external sources and by the electric current \mathbf{j} of the medium. Unlike the magnetic field, significant large-scale electric field in the conducting medium is absent in most cases (although not always) because of its shielding by the free electric charges.

The presence of the electric current and the magnetic field requires to modify the set of equations (2.1)–(2.5) in several ways, which converts it to a set of the **MHD equations**. The MHD is well suited for description of quasistationary electromagnetic phenomena in moving conducting plasma, either fully or partially ionized. It is worthwhile to emphasize that various plasma components (i.e., ions, electrons, neutrals, dust particles) must move together, composing a single “fluid”. Apparently, there are plenty natural phenomena when the electron and the ion components behave differently. Moreover, the plasma can contain many components, like ions of various elements in different ionization states, neutrals (atoms and molecules), relativistic particles and antiparticles, and the dust particles. To highlight this the classical MHD is frequently called the *one-fluid MHD*, in contrast to *two-fluid* or *multi-fluid* MHD, which consider the electrons, ions, and other available components as distinct fluids interacting with each other. The general multi-fluid approach is described in Sect. 1.3.3. Below we will return to considering corresponding generalizations of the one-fluid MHD as needed in appropriate chapters of this book. We start, however, from the phenomena allowing correct treatment within the standard one-fluid MHD.

As mentioned (see Sect. 1.3.3) the MHD description is an approximation to a more precise kinetic treatment of the plasma. Complementary, the MHD theory represents a generalization of the standard HD to the case of the conducting fluid; here we discuss how this generalization can be performed. To convert the HD into MHD equations, we first have to add the volume *Ampère force*

$$\mathbf{f}_A = \frac{1}{c} \mathbf{j} \times \mathbf{B}, \quad (2.10)$$

to equation of motion (2.2) and the Joule losses

$$Q = \frac{j^2}{\sigma} \quad (2.11)$$

to equation of the entropy balance (2.4). Second, we have to add the entire set of the Maxwell equations in the form

$$\nabla \times \mathbf{B} = \frac{4\pi}{c} \mathbf{j}, \quad \nabla \cdot \mathbf{B} = 0, \quad \frac{\partial \mathbf{B}}{\partial t} = -c \nabla \times \mathbf{E}, \quad (2.12)$$

where, unlike Sect. 1.3.3, we do not consider the external current \mathbf{j}^{ext} . We have already taken into account inequalities (2.9), which must hold for the magnetic field like for the standard HD variables in Sect. 2.1, i.e., we discarded the displacement current from the first equation in set (2.12) since it is small compared with the conductivity current in the slow phenomena described within the MHD approach.

Eliminating electric current \mathbf{j} from Eq. (2.10) with the use of the first of equations (2.12), we obtain MHD equations containing the magnetic field:

$$\rho \left(\frac{\partial \mathbf{u}}{\partial t} + (\mathbf{u} \cdot \nabla) \mathbf{u} \right) = -\nabla p + \mathbf{f} + \frac{1}{4\pi} [\nabla \times \mathbf{B}] \times \mathbf{B} + \eta \Delta \mathbf{u} + \frac{\eta}{3} \nabla (\nabla \cdot \mathbf{u}), \quad (2.13a)$$

$$\begin{aligned} \rho T \left(\frac{\partial s}{\partial t} + (\mathbf{u} \cdot \nabla) s \right) &= \eta \left(\frac{\partial u_\alpha}{\partial x_\beta} + \frac{\partial u_\beta}{\partial x_\alpha} - \frac{2}{3} (\nabla \cdot \mathbf{u}) \delta_{\alpha\beta} \right) \nabla_\beta u_\alpha + \nabla \cdot (\chi \nabla T) \\ &\quad + \frac{\nu_m}{4\pi} [\nabla \times \mathbf{B}]^2 \end{aligned} \quad (2.13b)$$

from original HD equations (2.2) and (2.4) complemented by Eqs. (2.10) and (2.11). Note that the first term in the rhs of Eq. (2.13b) can be expressed via viscous stress tensor $\Pi_{\alpha\beta}$ (2.5). Remaining equations (2.1), (2.3), and (2.5) keep the original form and so we just add them to Eq. (2.13) toward the closed MHD equation set.

The equations obtained so far do not compose the closed system yet, since the magnetic field is still undefined within it. To calculate the magnetic field we have to eliminate the electric field from Maxwell equations (2.12) with the use of Ohm's law—the relation between electric current and electromagnetic field. In a general case this law is very complicated (so-called generalized Ohm's law; see Sect. 1.3.4); we first consider the simplest case of Ohm's law. The motion of a conductor with a nonrelativistic speed $u \ll c$ in the presence of magnetic field \mathbf{B} gives rise to an additional electric field $\mathbf{u} \times \mathbf{B}/c$ in the conductor (see the Lorentz transformation, Landau and Lifshitz 1960). Thus, Ohm's law takes the form

$$\mathbf{j} = \sigma \left(\mathbf{E} + \frac{1}{c} \mathbf{u} \times \mathbf{B} \right), \quad (2.14)$$

where σ is the electric conductivity. This expression is valid when the magnetic field is relatively weak; otherwise the conductivity becomes essentially anisotropic [i.e., σ is a tensor rather than a scalar; see expressions (1.102)] and when there are no currents produced by the conductor nonuniformity (related to gradients of temperature or density). Current density (2.14) is the same in both the conductor (moving) and laboratory (rest) reference systems to the first order over u/c .

Let us make further transformations required to derive the equation for the magnetic field. First, express the electric field \mathbf{E} from Eq. (2.14),

$\mathbf{E} = \mathbf{j}/\sigma - \mathbf{u} \times \mathbf{B}/c$, and substitute it into the third equation of set (2.12), the **induction equation**. Then, the use of the relation

$$\Delta \mathbf{B} = -\frac{c}{4\pi} \nabla \times \mathbf{j}, \quad (2.15)$$

which follows from the first two equations of set (2.12), gives rise to equation linking the magnetic field with the motion of the medium:

$$\nabla \cdot \mathbf{B} = 0, \quad \frac{\partial \mathbf{B}}{\partial t} = \nabla \times [\mathbf{u} \times \mathbf{B}] + \nu_m \Delta \mathbf{B}, \quad \nu_m = \frac{c^2}{4\pi\sigma} = \text{const.} \quad (2.16)$$

The quantity ν_m is called the **magnetic diffusivity** or magnetic viscosity. Thus, finite conductivity gives rise to a dissipative process—the Joule dissipation of the magnetic field.

2.2.1 Magnetic Pressure and Magnetic Tensions

Consider now a few concepts and ideas, which follow from the full MHD system and so are the most widely applicable. First, we note that the magnetic Ampère force entering (2.13a) can be equivalently expanded onto two terms $[\nabla \times \mathbf{B}] \times \mathbf{B} = -\nabla B^2/2 + (\mathbf{B} \cdot \nabla) \mathbf{B}$ with the use of the corresponding equivalence of the vector analysis. As a result, part of the magnetic force reveals itself as the gradient of a **magnetic pressure** $p_m = B^2/8\pi$, which adds up to the kinematic gas pressure p :

$$\begin{aligned} \frac{\partial \mathbf{u}}{\partial t} + (\mathbf{u} \cdot \nabla) \mathbf{u} &= -\frac{1}{\rho} \nabla \left(p + \frac{B^2}{8\pi} \right) + \frac{1}{4\pi\rho} (\mathbf{B} \cdot \nabla) \mathbf{B} \\ &\quad + \nu \Delta \mathbf{u} + \frac{\nu}{3} \nabla (\nabla \cdot \mathbf{u}) + \frac{1}{\rho} \mathbf{f}, \end{aligned} \quad (2.17)$$

while the other part forms the **magnetic tensions** $(\mathbf{B} \cdot \nabla) \mathbf{B}/4\pi\rho$, which have a nonzero value only when the magnetic field lines have a curved shape. Direct comparison of Eqs. (2.16) and (2.17) shows that the magnetic diffusivity ν_m plays the same role for the magnetic field as the kinematic viscosity ν plays for the hydrodynamic velocity \mathbf{u} .

2.2.2 Ideal MHD Equations

Ideal MHD equation set similar to set (2.7a) in the standard HD can be derived by neglecting the dissipative terms throughout the MHD equation system:

$$\frac{\partial \rho}{\partial t} + \nabla \cdot (\rho \mathbf{u}) = 0, \quad (2.18a)$$

$$\frac{\partial \mathbf{u}}{\partial t} + (\mathbf{u} \cdot \nabla) \mathbf{u} = -\frac{1}{\rho} \nabla \left(p + \frac{B^2}{8\pi} \right) + \frac{1}{4\pi\rho} (\mathbf{B} \cdot \nabla) \mathbf{B} + \frac{1}{\rho} \mathbf{f}, \quad (2.18b)$$

$$\frac{\partial s}{\partial t} + (\mathbf{u} \cdot \nabla) s = 0, \quad p = p(\rho, s), \quad (2.18c)$$

$$\frac{\partial \mathbf{B}}{\partial t} = \nabla \times [\mathbf{u} \times \mathbf{B}], \quad \nabla \cdot \mathbf{B} = 0. \quad (2.18d)$$

Apparently, this system is valid if the MHD parameters vary slowly in space and time and when the dissipation is weak. The electric field in this case can be expressed via the magnetic field and the medium velocity. Indeed, adopting $\sigma \rightarrow \infty$ in Eq. (2.14) and assuming the current density \mathbf{j} to remain finite we immediately obtain

$$\mathbf{E} = -\frac{1}{c} \mathbf{u} \times \mathbf{B}. \quad (2.19)$$

2.2.3 Quiescent Prominence Model

Figure 1.2 offers an idea of a prominence often observed in the solar corona. In fact, prominences represent relatively cool, $T \sim 10^4$ K, and dense $n \sim 10^{10} - 10^{11} \text{ cm}^{-3}$ partly ionized condensations (filaments) with the size exceeding 10^{10} cm , which can live high in the corona remarkably long, up to a few months, without immediately falling onto the photosphere, although the gravitational force would imply so. Kippenhahn and Schlüter (1957) noted that in certain magnetic configurations the gravitational force can be entirely compensated by the magnetic forces considered above. Let us consider a simple one-dimensional model of a quiescent prominence proposed by Kippenhahn and Schlüter (1957).

Specifically, we adopt that all relevant variables depend only on coordinate x : $\rho(x)$, $p(x)$, and $B_z(x)$, while other magnetic field components, B_x and

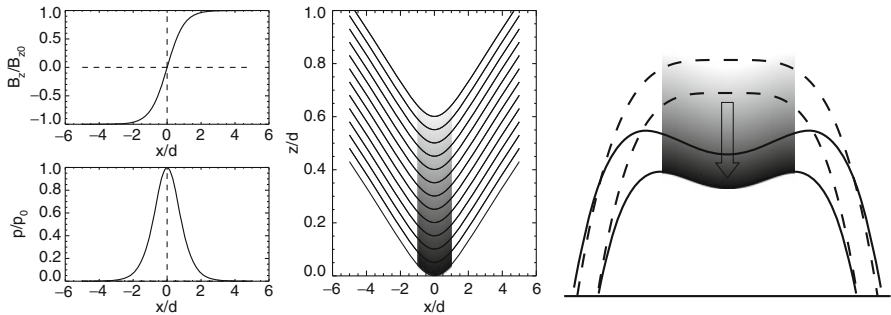


Figure 2.1: *Left*: Kippenhahn–Schlüter solution for the vertical magnetic field, pressure, and the field line structure. *Right*: a cartoon of the prominence/filament formation due to coronal condensation and corresponding magnetic field line distortion; see Aschwanden (2005) for more detail.

B_y and temperature T , are constant. In a steady state the lhs of Eq. (2.18b) is, apparently, zero; thus, projections of the rhs onto x and z axes yield

$$\frac{\partial}{\partial x} \left(p + \frac{B^2}{8\pi} \right) = 0, \quad (2.20a)$$

$$\frac{B_x}{4\pi} \frac{\partial B_z(x)}{\partial x} - \rho g = 0, \quad (2.20b)$$

where g is the free-fall acceleration. To solve the first of these equation we have yet to specify boundary conditions at the infinities, for which we adopt

$$p|_{x \rightarrow \pm\infty} = 0; \quad B_z|_{x \rightarrow \pm\infty} = \pm B_{z0}, \quad (2.21)$$

then, integration of Eq. (2.20aa) yields

$$p(x) = \frac{B_{z0}^2 - B_z^2(x)}{8\pi}. \quad (2.22)$$

Now we have to express the mass density ρ entering Eq. (2.20ab) via the gas pressure using the ideal gas equation of state:

$$p = 2n_e k_B T_e; \quad n_e = \rho / m_{\text{eff}}, \quad (2.23)$$

where m_{eff} is the mean mass of the coronal ions; thus, $\rho = pm_{\text{eff}} / (2k_B T_e)$.

Substituting this density into Eq. (2.20), then using solution (2.22) for the pressure, and noting that the constant combination $2k_B T_e / (gm_{\text{eff}})$ has a dimension of length (which is, in fact, the pressure scale height of a steady atmosphere, $\lambda_p = 2k_B T_e / (gm_{\text{eff}}) = 4.6 \times 10^9 (T_e / 1 \text{ MK}) \text{ cm}$), we obtain a closed form of equation for the magnetic field component $B_z(x)$:

$$\frac{B_{z0}^2 - B_z^2(x)}{2\lambda_p} - B_x \frac{\partial B_z(x)}{\partial x} = 0, \quad (2.24)$$

whose solution has an analytical form:

$$B_z(x) = B_{z0} \tanh \left(\frac{x B_{z0}}{2\lambda_p B_x} \right); \quad (2.25)$$

accordingly, the pressure distribution receives the form:

$$p(x) = \frac{B_{z0}^2}{8\pi} \cosh^{-2} \left(\frac{x B_{z0}}{2\lambda_p B_x} \right). \quad (2.26)$$

This solution illustrated by Fig. 2.1 implies that the magnetic pressure and the magnetic tensions are capable of compensating the gravitation force acting from the Sun to the coronal material. In particular, it can support some overdense coronal condensations observed in the form of bright prominences above the limb or as dark, compared with the photosphere, elongated filaments on the solar disk. Some of the observed filaments are indeed quiescent and can be approximately described using the presented Kippenhahn–Schlüter solution, while others are unstable eruptive structures, which are, apparently, not steady-state objects, so their description requires a dynamical approach; see Aschwanden (2005) for greater detail.

2.3 Diffusion, Reconnection, and Freezing-in of the Magnetic Field

Consider the equations for the magnetic field in more detail. First of all we note that two terms in the rhs of induction equation (2.16) have different structure and so describe different physical phenomena. First of them describes transport of the magnetic field by the plasma motion, while the second one describes the Joule dissipation of the field. The order of magnitude estimate of the first to the second term ratio yields the dimensionless parameter:

$$R_m = \frac{ul}{\nu_m}, \quad (2.27)$$

having the same structure as Reynolds number (2.6) and called the **magnetic Reynolds number**. This estimate assumes that the characteristic scales of magnetic field and velocity are the same and equal l .

2.3.1 Diffusion of the Magnetic Field

The type of solution of Eq. (2.16) depends essentially on the magnetic Reynolds number. If $R_m \ll 1$ we can neglect any motion of the plasma and so neglect the first term in the rhs of Eq. (2.16). Assume $R_m \ll 1$ and consider the problem of the magnetic field evolution in the infinite uniform conducting medium. Adopt that at $t = 0$ there is a magnetic field $\mathbf{B}(\mathbf{r}, 0) = \mathbf{B}_0(\mathbf{r})$ in the medium and find its evolution afterward for $t > 0$.

To solve the equation let us include the initial condition in the equation itself:

$$\frac{\partial \mathbf{B}}{\partial t} - \nu_m \Delta \mathbf{B} = \mathbf{B}_0(\mathbf{r})\delta(t), \quad \mathbf{B} = 0 \quad \text{at} \quad t < 0. \quad (2.28)$$

To make sure that Eq. (2.28) is equivalent to the original equation with the initial condition, we integrate both sides of it over a small time interval, $(-\tau, +\tau)$. If $\tau \rightarrow 0$ then $\mathbf{B}(\mathbf{r}, 0) = \mathbf{B}_0(\mathbf{r})$, because $\tau \Delta \mathbf{B} \rightarrow 0$ and so the second term in the lhs vanishes. Unlike Eq. (2.16), equation (2.28) is inhomogeneous and thus it can be solved using the Green function method:

$$\mathbf{B}(\mathbf{r}, t) = \int G(\mathbf{r} - \mathbf{r}', t - t') \mathbf{B}_0(\mathbf{r}') \delta(t') d^3 r' dt' = \int G(\mathbf{r} - \mathbf{r}', t) \mathbf{B}_0(\mathbf{r}') d^3 r', \quad (2.29)$$

where the **Green function** $G(\mathbf{r} - \mathbf{r}', t - t')$ satisfies the equation

$$\frac{\partial G}{\partial t} - \nu_m \Delta G = \delta(\mathbf{r} - \mathbf{r}') \delta(t - t'), \quad G = 0 \quad \text{at} \quad t - t' < 0. \quad (2.30)$$

Equation (2.30) can easily be solved by expansion of the Green function into Fourier integral over spatial variable $\mathbf{r} - \mathbf{r}'$. Apparently, its Fourier

transform G_k satisfies the equation

$$\frac{\partial G_k}{\partial t} + \nu_m k^2 G_k = \delta(t - t'), \quad (2.31)$$

which has the solution $G_k(t - t') = \Theta(t - t')e^{-\nu_m(t-t')k^2}$. The inverse Fourier transform yields the Green function in the spatial and temporal domain:

$$G(\mathbf{r} - \mathbf{r}', t - t') = \int G_k(t - t') e^{i\mathbf{k} \cdot (\mathbf{r} - \mathbf{r}')} \frac{d^3k}{(2\pi)^3} = \frac{\Theta(t - t')}{[4\pi\nu_m(t - t')]^{3/2}} \exp \left\{ -\frac{(\mathbf{r} - \mathbf{r}')^2}{4\nu_m(t - t')} \right\}, \quad (2.32)$$

where $\Theta(t - t')$ is the *step function*.

The structure of the exponent in Green function (2.32) shows explicitly that in the MHD (quasistationary) approximation, the magnetic field in a conducting medium propagates distance l over time $\Delta t \approx l^2/4\nu_m$. This is the very same law which describes the heat propagation or particle diffusion in a classical medium at rest. Accordingly, we can interpret the obtained solution as *diffusion of the magnetic field*; this is why the coefficient ν_m is called “magnetic diffusivity”. Considering an AC field with frequency ω , we take $\Delta t \approx T/2 = \pi/\omega$, which gives rise to a characteristic scale $L \approx c/\sqrt{\sigma\omega}$, providing an order of magnitude estimate of the skin depth of a conductor into which an external AC field can penetrate.

2.3.2 Freezing-in of the Magnetic Field and Magnetic Reconnection

Consider now the case of large Reynolds number, $R_m \gg 1$, when we can safely discard the Joule dissipation term:

$$\frac{\partial \mathbf{B}}{\partial t} = \nabla \times [\mathbf{u} \times \mathbf{B}], \quad \nabla \cdot \mathbf{B} = 0. \quad (2.33)$$

Let us show that under this condition the magnetic field has a remarkable property of *freezing-in* in the well-conducting fluid, i.e., any field line remains strictly linked with those macroscopic volume elements of the plasma, which contained it originally. Stated another way, the magnetic field is transferred along with the plasma motions; the magnetic field lines can change the length and shape, but cannot intersect and move through each other.

To see this explicitly, consider two *fluid particles* (i.e., two macroscopically small-volume elements of the plasma), which are located in nearby positions with the coordinates \mathbf{r} and $\mathbf{r} + \delta\mathbf{l}$ with the velocities \mathbf{u} and $\mathbf{u} + (\delta\mathbf{l} \cdot \nabla)\mathbf{u}$, respectively. Apparently, over the time interval dt , the distance between the particles changes by $(\delta\mathbf{l} \cdot \nabla)\mathbf{u}dt$; thus, this variation obeys the equation:

$$\frac{d}{dt} \delta\mathbf{l} = (\delta\mathbf{l} \cdot \nabla)\mathbf{u}. \quad (2.34)$$

The lhs contains the material derivative as it describes variation of the distance between two moving particles.

Complementary, calculate the material derivative of the \mathbf{B}/ρ ratio. This derivative reads:

$$\frac{d}{dt} \frac{\mathbf{B}}{\rho} = \frac{1}{\rho} \frac{d\mathbf{B}}{dt} - \frac{\mathbf{B}}{\rho^2} \frac{d\rho}{dt}. \quad (2.35)$$

The material derivative of the field \mathbf{B} is obtained from Eq. (2.33) taking into account the following transformation $\nabla \times [\mathbf{u} \times \mathbf{B}] = \mathbf{u}(\nabla \cdot \mathbf{B}) - \mathbf{B}(\nabla \cdot \mathbf{u}) - (\mathbf{u} \cdot \nabla)\mathbf{B} + (\mathbf{B} \cdot \nabla)\mathbf{u} = -(\mathbf{u} \cdot \nabla)\mathbf{B} + (\mathbf{B} \cdot \nabla)\mathbf{u} - \mathbf{B}(\nabla \cdot \mathbf{u})$:

$$\frac{d\mathbf{B}}{dt} = (\mathbf{B} \cdot \nabla)\mathbf{u} - \mathbf{B}(\nabla \cdot \mathbf{u}). \quad (2.36)$$

The material derivative of the density is obtained from continuity equation (2.1):

$$\frac{d\rho}{dt} = -\rho(\nabla \cdot \mathbf{u}). \quad (2.37)$$

Combining equations (2.35)–(2.37), we find

$$\frac{d}{dt} \frac{\mathbf{B}}{\rho} = \left(\frac{\mathbf{B}}{\rho} \cdot \nabla \right) \mathbf{u}. \quad (2.38)$$

Equations (2.34) and (2.38) for the variables $\delta \mathbf{l}$ and \mathbf{B}/ρ are identical. Therefore, if these two fluid particles were originally connected by a field line, i.e., the vectors $\delta \mathbf{l}$ and \mathbf{B}/ρ were parallel to each other, they remain parallel at all later times; thus, the particles remain linked to the same field line. During the plasma motion, the magnitude \mathbf{B}/ρ is changing proportionally to the distance between the particles. In particular, the freezing-in property guarantees conservation of the magnetic flux through arbitrary closed moving contour composed of the fluid elements of the medium.

It is important to emphasize that the flux conservation holds for *arbitrary* macroscopic motions and deformations of the contour *compatible* with the condition $R_m \gg 1$. This means that if in a fluid with overall large Reynolds number there are inhomogeneous regions where the spatial gradients are extraordinary large, the freezing-in condition can break down there allowing the magnetic field to diffuse locally. Given that the field is freezing in the fluid in the most of the volume, while diffuses only in some locally inhomogeneous regions, this magnetic field dissipation process will macroscopically look like a reconnection of magnetic field lines. Stated another way, dissipation of magnetic energy in a highly conducting fluid with large Reynolds numbers can only occur in the form of **magnetic reconnection**, which requires some strong local inhomogeneities to be present in the fluid.

2.3.3 Stationary Configurations

Let us discuss briefly what requirements must be fulfilled to allow a stationary MHD configuration—stationary plasma motion or stationary magnetic field configuration. Stationary solution implies $\partial/\partial t = 0$ in Eq. (2.13), so neglecting the dissipative terms, one easily finds $s = \text{const}$ from Eq. (2.13b), while Eq. (2.13a) describes the force balance

$$\rho(\mathbf{u} \cdot \nabla) \mathbf{u} = -\nabla p - \frac{1}{4\pi} \mathbf{B} \times [\nabla \times \mathbf{B}], \quad (2.39)$$

i.e., the inertia force, $\rho(\mathbf{u} \cdot \nabla) \mathbf{u}$, must be balanced by the pressure gradient ∇p and the Ampère force $\mathbf{f}_A = -\mathbf{B} \times [\nabla \times \mathbf{B}]/(4\pi)$; we do not consider a gravitational force here for simplicity. The order of magnitude of each term can be estimated if we introduce a characteristic scale of the spatial variation of the involved parameters, $\nabla \sim l^{-1}$:

$$\frac{\rho u^2}{l} \approx \frac{p}{l} + \frac{B^2}{4\pi l}, \quad \text{or} \quad \rho u^2 \approx p + \frac{B^2}{4\pi}. \quad (2.40)$$

Consider the case of strong pressure, $p \gg B^2/(4\pi)$. Here one can neglect the Ampère force in Eq. (2.39) in the first approximation, so the inertia force of the plasma flow $\mathbf{u}(\mathbf{r})$ is balanced by the pressure gradient. Stated another way, in a high-pressure plasma, the effect of the magnetic field on the stationary plasma flow is minor and solutions of usual HD apply. The magnetic field configuration then can be determined within the perturbation theory for a given HD flow. In particular, the magnetic field, being frozen in the plasma, is simply transferred with the predefined plasma motion. As we will show, however, in Chaps. 6 and 8, such a weak magnetic field might be kinematically amplified by plasma motions, so the stationary flows with weak magnetic field are not necessarily stable.

The opposite case of strong magnetic field, $B^2/(4\pi) \gg p$, is more complicated. Indeed, if we neglect the pressure gradient in Eq. (2.39), we arrive at two options: either the plasma flow is highly supersonic, $\rho u^2 \gg p$, or the magnetic field creates relatively small Ampère's force, $|\mathbf{B} \times [\nabla \times \mathbf{B}]| \ll B^2/l$; ultimately, this condition requires that the electric current $\mathbf{j} = c[\nabla \times \mathbf{B}]/(4\pi)$ is almost parallel to the magnetic field \mathbf{B} .

The former case is thought to be realized in so-called Poynting-dominated jets. Collimated supersonic (often relativistic) jets are widely detected or implied in astrophysical sources including active galactic nuclei, quasars and microquasars, and the gamma-ray burst sources; see Sect. 12.4. It is yet unclear, however, if those jets are pressure-dominated or Poynting-dominated.

The latter case, which is called the force-free field, because in the first approximation the Ampère force must be zero here, seems to be relevant to coronae of accretion disks and normal stars including the solar corona. For the solar corona, for example, the sources of the coronal magnetic field

are located at and beneath the photosphere, and so the magnetic pressure can strongly dominate the kinetic pressure at the active regions above the sunspots, where the photospheric field is highly enhanced compared with the mean photospheric magnetic field. The corresponding magnetic configurations are indeed routinely observed in the solar corona to be stationary and to survive over a few solar rotations with very little evolution.

Currently, there is no reliable routine method to measure coronal magnetic fields. For this reason, different force-free extrapolations of the photospheric magnetic fields, which are widely measured with the use of Zeeman effect, are developed and used to deduce some information on the coronal fields. Although the extrapolation techniques are very useful to get some idea on the coronal fields, the extrapolated magnetic structures often do not match any observed coronal structure. One of possible reason for those mismatches is that the magnetic field is in fact only approximately the force-free field.

To quantify the accuracy of the force-free approximation, assume that the plasma obeys the ideal gas equation of state, Eq. (2.23), $p = 2nT$, where temperature T is measured in energy units ($T = k_B T$ [K]), and introduce the *plasma beta* parameter

$$\beta = \frac{4\pi p}{B^2} = \frac{8\pi nT}{B^2} = \frac{w_T}{w_B}, \quad (2.41)$$

where $w_T = nT$ and $w_B = B^2/(8\pi)$ are the densities of the thermal and magnetic energies, respectively. Thus, for the magnetic-dominated (low beta) plasma, the Ampère force equals zero not equivalently but to the accuracy of β only: $|\mathbf{B} \times [\nabla \times \mathbf{B}]| \sim \beta B^2/l$, which may have noticeable effect on the accuracy of the force-free photospheric extrapolations. To get a better feeling about the numbers involved, let us estimate the plasma beta in the solar corona—in and outside an active region. Outside active regions we can adopt the typical values $B \sim 1$ G, $n \sim 10^8 \text{ cm}^{-3}$, and $T \sim 1$ MK, which yields an estimate about one: $\beta \sim 0.4$. In an active region above a sunspot, the magnetic field can be much larger, $B \sim 100$ G or higher, and the plasma can be denser, $n \sim 10^{10} \text{ cm}^{-3}$, and hotter, $T \sim 3\text{--}10$ MK, so a small $\beta \lesssim 10^{-2}$ is typically expected.

Overall, we conclude that the magnetic configurations and plasma flows can be essentially different in the pressure-dominated ($\beta \gg 1$) and the magnetic-dominated ($\beta \ll 1$) plasmas—this is, in fact, relevant to both stationary and nonstationary cases.

2.4 Linear Modes in MHD

An arbitrary perturbation in a plasma can be expanded over any full system of orthogonal functions. The most convenient set of such functions, however, is the set of linear eigenmodes of the medium. Indeed, for a small-amplitude

perturbation, the amplitudes of the individual eigenmodes composing it are also small; thus, the superposition principle valid for the linear systems applies and so the individual eigenmodes do not interact with each other. Even for larger-amplitude perturbations the representation over the eigenmode superposition is frequently very useful, since, for a small nonlinearity, the nonlinear interactions of the linear eigenmodes can be taken into account by the perturbation theory. The role of the linear modes is also very important to study plasma instabilities. Therefore, we discuss now the MHD eigenmodes of the plasma.

2.4.1 Basic Equations and MHD Dispersion Relation

To study small-amplitude MHD waves in a fully ionized plasma (low-frequency plasma eigenmodes, $\mathbf{j}^{\text{ext}} = 0$), we have to analyze the corresponding linearized set of equations. We start with a non-dissipative case ($\nu_m = \nu_{\text{eff}} = 0$, $\tilde{S} = 0$) and use Eqs. (1.134)–(1.136) keeping the Hall term in Eq. (1.134). We represent the macroscopic plasma parameters in the form $\mathbf{U} = \mathbf{U}_0 + \mathbf{u}$, $s = s_0 + s'$, etc., where the index 0 designates the unperturbed values of quantities which do not depend on coordinates and time; small perturbations will be considered in the linear approximation only. Linearizing the system of MHD equations with these notations yields

$$\frac{\partial s'}{\partial t} + \mathbf{U}_0 \cdot \nabla s' = 0, \quad \frac{\partial \rho'}{\partial t} + \mathbf{U}_0 \cdot \nabla \rho' + \rho_0 \nabla \cdot \mathbf{u} = 0, \quad (2.42a)$$

$$\frac{\partial \mathbf{u}}{\partial t} + (\mathbf{U}_0 \cdot \nabla) \mathbf{u} + \frac{1}{\rho_0} \nabla p + \frac{1}{4\pi\rho_0} \mathbf{B}_0 \times (\nabla \times \mathbf{b}) = 0, \quad P = P_0 + p(s', \rho'), \quad (2.42b)$$

$$\frac{\partial \mathbf{b}}{\partial t} + (\mathbf{U}_0 \cdot \nabla) \mathbf{b} + \mathbf{B}_0 (\nabla \cdot \mathbf{u}) - (\mathbf{B}_0 \cdot \nabla) \mathbf{u} + \frac{c}{4\pi en_i} (\mathbf{B}_0 \cdot \nabla) (\nabla \times \mathbf{b}) = 0, \quad \nabla \cdot \mathbf{b} = 0. \quad (2.42c)$$

We search for solutions of this system having the form of plane monochromatic waves $s' \propto \exp(i\mathbf{k} \cdot \mathbf{r} - i\omega t)$ and obtain the set of algebraic equations:

$$\omega' s' = 0, \quad \omega' \rho' - \rho_0 \mathbf{k} \cdot \mathbf{u} = 0, \quad (2.43a)$$

$$\omega' \mathbf{u} - \frac{\mathbf{k}}{\rho_0} \left(p + \frac{\mathbf{b} \cdot \mathbf{B}_0}{4\pi} \right) + \frac{\mathbf{k} \cdot \mathbf{B}_0}{4\pi\rho_0} \mathbf{b} = 0, \quad p = c_s^2 \rho' + \left(\frac{\partial P}{\partial s} \right)_{\rho_0} s', \quad (2.43b)$$

$$\omega' \mathbf{b} + (\mathbf{k} \cdot \mathbf{B}_0) \mathbf{u} - \mathbf{B}_0 (\mathbf{k} \cdot \mathbf{u}) - i \frac{c \mathbf{k} \cdot \mathbf{B}_0}{4\pi en_i} \mathbf{k} \times \mathbf{b} = 0, \quad \mathbf{k} \cdot \mathbf{b} = 0, \quad (2.43c)$$

where $c_s^2 = (\partial P / \partial \rho)_0$ is the square of the unperturbed sound velocity; $\omega' = \omega - \mathbf{k} \cdot \mathbf{U}_0$ is the frequency in the co-moving system, which experiences a Doppler shift relative to its frequency in the laboratory reference frame. System (2.43) is a set of linear homogeneous equations and so it has a nontrivial

solution only when the determinant of the system is zero. Neglecting the Hall term, the determinant is derived, e.g., in Somov (2006):

$$\omega'^2[\omega'^2 - (\mathbf{k}\mathbf{v}_A)^2][\omega'^4 - k^2(c_s^2 + v_A^2)\omega'^2 + k^2c_s^2(\mathbf{k}\mathbf{v}_A)^2] = 0,$$

where $v_A = B_0/\sqrt{4\pi\rho_0}$ is the **Alfvén speed**. This equation can have four nonnegative roots, describing four linear MHD modes, which we consider below in more detail. In what follows, complementary to Somov (2006) analysis, we derive properties of the small-amplitude waves directly from the full system (with the Hall term) without explicit use of the determinant.

2.4.2 Dispersion and Polarization of Linear Modes

Hydrodynamics Case: $B_0 = 0$

Let us start from a simpler case, when no magnetic field is present in the plasma; $v_A = 0$. Then, the terms containing v_A drop out from the dispersion relation, which reduces to

$$\omega'^6(\omega'^2 - k^2c_s^2) = 0.$$

Evidently, this dispersion equation describes two distinct eigenmodes, corresponding to two its different solutions: $\omega' = 0$ and $\omega'^2 = k^2c_s^2$.

Entropy and Vortex Perturbations If we suppose in Eq. (2.43) that $B_0 = 0$ and $s' \neq 0$, we obtain $\omega' = 0$, i.e., $\omega = \mathbf{k} \cdot \mathbf{U}_0$. This means that entropy perturbations are motionless relative to the plasma and propagate with the velocity of the medium motion, \mathbf{U}_0 . Also, $\mathbf{k} \cdot \mathbf{u} = 0$, $\mathbf{k} \cdot \mathbf{b} = 0$, and $p = 0$, but the density perturbation $\rho' \neq 0$ and it is defined by s' .

Note that the root $\omega' = 0$ is triple degenerate, since it originates from equation $\omega'^6 = 0$. Therefore, two more eigenmodes must be present. Indeed, for $\omega' = 0$, the system (2.43) allows having nonzero values of the components \mathbf{u}_\perp and \mathbf{b}_\perp transverse to \mathbf{k} . Thus, in the general case $\mathbf{k} \times \mathbf{b} \neq 0$ and $\mathbf{k} \times \mathbf{u} \neq 0$, so, in addition to the entropy perturbation, there are two more vortex perturbations traveling with the plasma velocity, namely $\nabla \times \mathbf{b}$ and $\nabla \times \mathbf{u}$. In the absence of B_0 , they are independent from each other and from the perturbation of s' . It is interesting that even though no regular magnetic field is present in this case, the small perturbations of the magnetic field still can exist in the form of eddies ($\nabla \times \mathbf{b}$), which is a direct consequence of the fact that our linearized equations were obtained from more general MHD equations rather than from standard HD equations; in the latter case no magnetic perturbation would enter the linearized equations at all.

Sound Waves For $s' = 0$, perturbations oscillate with $\omega' \neq 0$. If, as before, $B_0 = 0$ then for $\omega' \neq 0$, it follows from Eq. (2.43) that $\mathbf{b} = 0$ and $\mathbf{u}_\perp = 0$,

but the perturbations u_{\parallel} and ρ' satisfy

$$\omega' \rho' - \rho_0 k u_{\parallel} = 0, \quad c_s^2 k \rho' - \rho_0 \omega' u_{\parallel} = 0, \quad (2.44)$$

which describes sound waves with the dispersion law

$$\omega'^2 = (c_s k)^2, \quad \omega = \pm c_s k + \mathbf{k} \cdot \mathbf{U}_0. \quad (2.45)$$

MHD Case: $B_0 \neq 0$

Entropy Perturbations in a Magnetic Field For $s' \neq 0$ and $\mathbf{k} \cdot \mathbf{B}_0 \neq 0$ we find from Eq. (2.43) that $\omega = \mathbf{k} \cdot \mathbf{U}_0$ and thus

$$\left(p + \frac{\mathbf{b} \cdot \mathbf{B}_0}{4\pi} \right) \mathbf{k} - \frac{\mathbf{k} \cdot \mathbf{B}_0}{4\pi} \mathbf{b} = 0. \quad (2.46)$$

Vector \mathbf{k} is orthogonal to \mathbf{b} , so Eq. (2.46) is equivalent to two equations:

$$(\mathbf{k} \cdot \mathbf{B}_0) \mathbf{b} = 0, \quad p + \frac{\mathbf{b} \cdot \mathbf{B}_0}{4\pi} = 0. \quad (2.47)$$

If $\mathbf{b} = 0$, $(\mathbf{k} \cdot \mathbf{B}_0) \neq 0$, we have from Eqs. (2.47) and (2.43) $\mathbf{u} = 0$, $p = 0$. Perturbations of the density and entropy are connected to each other by the condition $p = 0$.

If $\mathbf{b} \neq 0$, $(\mathbf{k} \cdot \mathbf{B}_0) = 0$, we obtain from Eq. (2.47) that perturbations of the full pressure are zero:

$$p + \frac{\mathbf{b} \cdot \mathbf{B}_0}{4\pi} = 0,$$

but in the general case $\rho' \neq 0$ and $p \neq 0$. It is easy to check that the vortex perturbations, $\nabla \times \mathbf{b}$ and $\nabla \times \mathbf{u}$, can exist now independently from s' and from each other. The simplest example of the entropy's perturbation is the transfer of heated cloud by medium motion.

Alfvén Waves Now we consider perturbations in which $s' = 0$ and $\rho' = 0$ but $\omega' \neq 0$. Constancy of mass density is the main generic attribute of the Alfvén waves. It follows from Eq. (2.43) that $\mathbf{b} \cdot \mathbf{B}_0 = 0$; i.e., $\mathbf{b} \perp \mathbf{B}_0$. Since $\mathbf{b} \perp \mathbf{k}$ as well, the perturbations are polarized, in the sense that \mathbf{b} is perpendicular to the plane $(\mathbf{k}, \mathbf{B}_0)$. The amplitudes \mathbf{u} and \mathbf{b} satisfy

$$\mathbf{u} = -\frac{\mathbf{k} \cdot \mathbf{B}_0}{4\pi \rho_0 \omega'} \mathbf{b}, \quad \mathbf{k} \cdot \mathbf{u} = 0, \quad (2.48a)$$

$$\omega' \mathbf{b} + (\mathbf{k} \cdot \mathbf{B}_0) \mathbf{u} - i \frac{c(\mathbf{k} \cdot \mathbf{B}_0)}{4\pi e n_i} \mathbf{k} \times \mathbf{b} = 0, \quad \mathbf{k} \cdot \mathbf{b} = 0. \quad (2.48b)$$

Excluding the velocity \mathbf{u} from Eq. (2.48b), we obtain

$$\left[\omega'^2 - \frac{(\mathbf{k} \cdot \mathbf{B}_0)^2}{4\pi\rho_0} \right] \mathbf{b} - i \frac{c\omega'(\mathbf{k} \cdot \mathbf{B}_0)}{4\pi en_i} \mathbf{k} \times \mathbf{b} = 0 \quad (2.49)$$

and further

$$\mathbf{k} \times \mathbf{b} = -i \frac{c\omega'k^2(\mathbf{k} \cdot \mathbf{B}_0)}{4\pi en_i(\omega'^2 - \omega_A^2)} \mathbf{b}, \quad \omega_A^2 = \frac{(\mathbf{k} \cdot \mathbf{B}_0)^2}{4\pi\rho_0}. \quad (2.50)$$

From last two equalities we find dispersion equation

$$\omega'^2 - \omega' \frac{\omega_A^2 k}{\omega_{\text{Bi}} k_{\parallel}} - \omega_A^2 = 0, \quad (2.51)$$

where $\rho_0 \approx m_i n_i$ and $\omega_{\text{Bi}} = eB_0/m_i c$ is the ion cyclotron frequency.

The solution of Eq. (2.51) is

$$\omega' = \omega_A [\xi \pm \sqrt{1 + \xi^2}], \quad \text{where} \quad \xi = \frac{\omega_A k}{2\omega_{\text{Bi}} k_{\parallel}} = \frac{(\mathbf{k} \cdot \mathbf{v}_A) k}{2\omega_{\text{Bi}} k_{\parallel}}. \quad (2.52)$$

Here the parameter $\xi = v_A k / 2\omega_{\text{Bi}}$ is expressed via the Alfvén velocity:

$$\mathbf{v}_A = \frac{\mathbf{B}_0}{\sqrt{4\pi\rho_0}}. \quad (2.53)$$

It is small, $\xi \ll 1$, if $k \ll 2\omega_{\text{Bi}}/v_A$ and $\lambda = 2\pi/k \gg v_A/\pi\omega_{\text{Bi}} = \lambda_c$. Note that parameter ξ is a result of accounting of the Hall current in the MHD equations. The scale λ_c is often small compared with other characteristic scales in astrophysics, which allows neglecting the corresponding Hall term. For example, in the “warm” phase of galactic disk $\lambda_c \approx 3 \times 10^7$ cm is even smaller than the gyroradius of thermal protons, $\approx 10^8$ cm, for $T \approx 1$ eV, $B_0 \approx 3 \mu\text{G}$; thus for certain plasmas the Hall term can be safely neglected in the entire range of the MHD applicability (recall that the MHD treatment is only correct if the wavelength is larger than the proton gyroradius).

Neglecting the small parameter ξ in Eq. (2.52) for $k \ll 2\omega_{\text{Bi}}/v_A$ we obtain simpler dispersion law for the Alfvén waves:

$$\omega' = \pm \frac{|\mathbf{k} \cdot \mathbf{B}_0|}{\sqrt{4\pi\rho_0}} = \pm |\mathbf{k} \cdot \mathbf{v}_g|, \quad (2.54)$$

where $\mathbf{v}_g = \pm \mathbf{v}_A$ is the group velocity of the Alfvén waves. Its phase velocity is

$$\mathbf{v}_{\text{ph}} = \pm \frac{B_0 |\cos \theta| \mathbf{k}}{\sqrt{4\pi\rho_0} k}, \quad (2.55)$$

where θ is the angle between \mathbf{k} and \mathbf{B}_0 . According to Eqs. (2.48a) and (2.54), the velocity \mathbf{u} and the magnetic field \mathbf{b} in the Alfvén wave are connected by a simple dependence:

$$\mathbf{u} = \mp \frac{\mathbf{b}}{\sqrt{4\pi\rho_0}}. \quad (2.56)$$

The minus sign in this formula refers to the same sign for ω' and $\mathbf{k} \cdot \mathbf{v}_A$, and the plus sign refers to different signs for their values. In Alfvén waves the curls $\nabla \times \mathbf{u}$ and $\nabla \times \mathbf{b}$ are not independent and both propagate with the Alfvén velocity relative to the plasma.

If the medium contains a significant portion of neutral atoms, the Alfvén velocity depends on the entire mass density $\rho \approx n_i m_i + n_a m_a$ only for the wavelengths $\lambda > \Lambda_{ia}$, where Λ_{ia} is the mean free path of the ions relative to collisions with the neutrals. In the case $\lambda < \Lambda_{ia}$ the motion of charged component is only weakly coupled with the motion of neutral atoms, so the true one-fluid description of the medium is not possible. The Alfvén waves with

$$\lambda \ll \Lambda_{ia}$$

may exist in the charged subsystem only, and the Alfvén velocity will be determined by the ion mass density alone, $\rho \approx n_i m_i$.

Magnetic Sound For $s' = 0$ but $\rho' \neq 0$ we find from Eq. (2.43) that

$$\omega' \rho' - \rho_0 \mathbf{k} \cdot \mathbf{u} = 0, \quad \mathbf{k} \cdot \mathbf{b} = 0, \quad (2.57a)$$

$$c_s^2 \mathbf{k} \rho' - \rho_0 \omega' \mathbf{u} + \frac{\mathbf{k}(\mathbf{B}_0 \cdot \mathbf{b})}{4\pi} - \frac{(\mathbf{k} \cdot \mathbf{B}_0) \mathbf{b}}{4\pi} = 0, \quad (2.57b)$$

$$(\mathbf{k} \cdot \mathbf{B}_0) \mathbf{u} - \mathbf{B}_0 (\mathbf{k} \cdot \mathbf{u}) + \omega' \mathbf{b} = 0. \quad (2.57c)$$

We again neglect here the Hall current, which is valid at low frequencies. Excluding the perturbation ρ' and multiplying Eqs. (2.57b) and (2.57c) by $\mathbf{e}_0 = \mathbf{B}_0/B_0$, we obtain two equations for the parallel components u_{\parallel} and b_{\parallel} :

$$\frac{c_s^2 k^2 B_0 k_{\parallel}}{4\pi \rho_0 (\omega'^2 - c_s^2 k^2)} b_{\parallel} - \omega' u_{\parallel} = 0, \quad (2.58a)$$

$$\frac{\omega'^2 - c_s^2 k^2 - v_A^2 k^2}{\omega'^2 - c_s^2 k^2} \omega' b_{\parallel} + B_0 k_{\parallel} u_{\parallel} = 0. \quad (2.58b)$$

Exclusion of u_{\parallel} leads to dispersion equation

$$\omega'^4 - \omega'^2 (c_s^2 + v_A^2) k^2 + c_s^2 v_A^2 k^4 \cos^2 \theta = 0, \quad (2.59)$$

where θ is the angle between \mathbf{B}_0 and \mathbf{k} . We find phase velocities $v = \omega'/k$ of the fast and slow magnetosonic modes from biquadratic Eq. (2.59):

$$v_{f,s}^2 = \frac{1}{2} \left[c_s^2 + v_A^2 \pm \sqrt{(c_s^2 + v_A^2)^2 - 4c_s^2 v_A^2 \cos^2 \theta} \right]. \quad (2.60)$$

Directions of the vectors \mathbf{b} and \mathbf{u} can easily be found from the above equations: \mathbf{b} belongs to the plane $(\mathbf{k}, \mathbf{B}_0)$ and perpendicular to the vector \mathbf{k} . The vector \mathbf{u} belongs to the same plane, but in general it has both components parallel and perpendicular to \mathbf{k} .

Transverse Propagation For $\mathbf{B}_0 \neq 0$ and $\mathbf{k} \perp \mathbf{B}_0$, Eq. (2.43) allows both entropy perturbations ($s' \neq 0$), considered above, and perturbations of the MHD parameters independent of the entropy variations. For $s' = 0$, the only nonzero component of \mathbf{u} is that parallel to \mathbf{k} , as for normal sound waves. As follows from Eq. (2.43), the magnitudes ρ' and $\mathbf{k} \cdot \mathbf{u}$ satisfy

$$\omega' \rho' - \rho_0 \mathbf{k} \cdot \mathbf{u} = 0, \quad -\frac{c_s^2 k^2 \rho'}{\rho_0} + \left(\omega' - \frac{v_A^2 k^2}{\omega'} \right) \mathbf{k} \cdot \mathbf{u} = 0. \quad (2.61)$$

From this, we determine the dispersion law for the transverse sound:

$$\omega' = \pm k (c_s^2 + v_A^2)^{1/2}. \quad (2.62)$$

The perturbations of the magnetic field are parallel to \mathbf{B}_0 and proportional to the density perturbations:

$$\mathbf{b} = \mathbf{B}_0 \frac{\rho'}{\rho_0}. \quad (2.63)$$

Thus, for transverse propagation, besides the entropy perturbations, it is possible to have only waves of the usual sound type, in which the velocity of the plasma is parallel to the direction of propagation. The sound velocity c_s is replaced by $(c_s^2 + v_A^2)^{1/2}$, i.e., it is renormalized by the magnetic field.

Longitudinal Propagation For $\mathbf{k} \parallel \mathbf{B}_0$ the system yields two types of wave in addition to the entropy perturbations: usual sound wave, described by Eqs. (2.46) and (2.47), on which the magnetic field has no influence, and MHD waves with \mathbf{u} and \mathbf{b} perpendicular to both directions $\mathbf{k} \parallel \mathbf{B}_0$. Excluding velocity

$$\mathbf{u}_\perp = \frac{(\mathbf{k} \mathbf{B}_0)}{4\pi \rho_0 \omega'} \mathbf{b}$$

from vector equations (2.43), we obtain

$$(\omega'^2 - \omega_A^2) \mathbf{e}_0 \times \mathbf{b} + i \frac{(\mathbf{k} \mathbf{B}_0) c k \omega'}{4\pi e n_i} \mathbf{b} = 0, \quad (2.64)$$

where ω_A is given by Eq. (2.50). Equation (2.64) can be written for the magnetic field components (b_x, b_y) , $\mathbf{b} = \mathbf{e}_x b_x + i \mathbf{e}_y b_y$ in the form

$$C_1 b_x - C_2 b_y = 0, \quad C_2 b_x - C_1 b_y = 0, \quad C_1 = \omega'^2 - \omega_A^2, \quad C_2 = \frac{(\mathbf{k} \mathbf{B}_0) c k \omega'}{4\pi e n_i}. \quad (2.65)$$

The determinant of this set of linear equations equals zero if $C_2^2 = C_1^2$, i.e., $b_y = \pm b_x$. This means that two MHD waves have the circular polarizations with opposite directions of rotation. The dispersion equation for MHD waves has the form

$$(\omega'^2 - \omega_A^2)^2 = \omega'^2 \omega_A^2 \left(\frac{ck}{\omega_{pi}} \right)^2, \quad \omega_{pi}^2 = \frac{4\pi e^2 n_i}{m_i}. \quad (2.66)$$

The waves have the frequencies $\omega' \approx \omega_A = \pm k B_0 / \sqrt{4\pi\rho_0}$, if contribution of the Hall current is small: $(ck/\omega_{pi})^2 \ll 1$.

The Full Set of Linear Modes With the account of the condition $\mathbf{k} \cdot \mathbf{b} = 0$, the last of equations (2.43) yields two equations when projected on the axes perpendicular to \mathbf{k} . The projection along \mathbf{k} gives the identity $0 = 0$. Together with the expression of p in terms of ρ' and s' , Eqs. (2.43) allow determining the following seven quantities: s' , ρ' , \mathbf{u} , and two components of \mathbf{b} . In the general case, as we have seen, there are seven different (and linearly independent) solutions: (1) entropy, (2) two Alfvén, (3) two fast, and (4) two slow magnetosonic waves, where the solutions differing in the sign of ω' are considered as different solutions. These solutions comprise the full system of linear eigenmodes over which any small perturbation can be expanded (Akhiezer et al. 1975).

Any perturbation of the MHD parameters leads to generation of one or another MHD mode, and therefore the excitation of modes in cosmic conditions may be highly diverse depending on the object. Sources of the MHD waves can include mechanical motions of the plasma, rapid transformations of energy (outbursts), hydrodynamic instabilities (convection), heating (solar and stellar winds), rotations, and so on. Secondary MHD modes are often generated by nonlinear interactions of MHD waves with each other or with different kinds of nonlinear perturbations (e.g., with shock waves). MHD modes may also be excited by external currents in the plasma, induced by external sources. Finally, there are purely kinetic mechanisms for excitation of MHD waves connected with the nonequilibrium distribution function of a plasma component. For example, strong nonequilibrium relativistic component (cosmic rays) is capable of generating MHD waves in the cosmic medium.

2.4.3 Damping of MHD Waves

We consider the most important conditions, when the MHD modes are long living, i.e., $\gamma \ll \omega'$, where γ is the wave damping rate. To investigate the MHD wave damping we use Eq. (1.129). The first term on the right-hand side of Eq. (1.129) is sign alternating and, therefore, goes to zero when averaged over the volume larger than $\lambda^3 = (2\pi/k)^3$. Systematic thermal dissipation Q

per unit volume is described by the positive quadratic terms in Eq. (1.129):

$$\begin{aligned}
 Q = T\dot{S} = & \frac{\chi(\nabla T)^2}{T} + \frac{1}{2}\rho_0\nu \left(\frac{\partial u_\alpha}{\partial x_\beta} + \frac{\partial u_\beta}{\partial x_\alpha} - \frac{2}{3}(\nabla \cdot \mathbf{u})\delta_{\alpha\beta} \right)^2 \\
 & + \frac{\nu_m}{4\pi} (\nabla \times \mathbf{b})_\parallel^2 + \frac{\nu_{\text{eff}}}{4\pi} (\nabla \times \mathbf{b})_\perp^2.
 \end{aligned} \tag{2.67}$$

The thermal dissipation includes three distinct dissipative processes: heat conductivity, viscosity, and Joule heating.

The damping rate γ , which describes a weak damping of the plane monochromatic waves in stationary plasma, can be calculated from

$$\gamma = \overline{Q}/2\overline{w}, \tag{2.68}$$

where w is the density of the wave energy; the bar over it indicates the mean amplitude over the period. The magnitude of γ describes exponential damping of MHD parameters when all the wave sources are off, e.g., $\mathbf{u} = \mathbf{u}_0 \exp(-\gamma t)$ or $\overline{w} \propto \exp(-2\gamma t)$ for quadratic measures like the energy density.

Another kind of damping measures is the absorption coefficient per unit path length of the wave propagation:

$$\alpha = \overline{Q}/\overline{q}, \tag{2.69}$$

where \overline{q} is the mean absolute value of the wave energy flux. This value characterizes exponential decrease of the wave amplitude in space, $\mathbf{u} = \mathbf{u}_0 \exp(-\alpha z)$, as the wave propagates from the source. Here, we select the z -axis along the direction of the energy flux $\overline{\mathbf{q}}$. The general expressions for energy density and energy flux density are well known (Landau and Lifshitz 1966; see also Sect. 1.3.3):

$$w = \rho \left(\frac{1}{2}u^2 + \epsilon \right) + \frac{B^2}{8\pi}, \tag{2.70a}$$

$$\mathbf{q} = \rho \mathbf{u} \left(\frac{1}{2}u^2 + \epsilon + \frac{P}{\rho} \right) + \frac{1}{4\pi} \mathbf{B} \times (\mathbf{u} \times \mathbf{B}), \tag{2.70b}$$

where ϵ is the internal energy per unit mass and $\epsilon + P/\rho$ is the enthalpy. This energy flux does not include the dissipative terms.

It is now easy to apply these general formulae to derive the damping rates of the MHD waves; we list the final results only for the sake of brevity.

Sound Waves: $B_0 = 0$

$$\gamma_s = \frac{1}{2}k^2 \left[\frac{4}{3}\nu + \frac{\chi}{\rho}(c_V^{-1} - c_P^{-1}) \right], \tag{2.71}$$

where c_V and c_P are the specific heats at constant volume and pressure, respectively. The absorption coefficient per unit path length is $\alpha_s = \gamma_s/c_s$, where c_s is the group velocity of the sound wave.

Alfvén Waves

$$\gamma_A = \frac{1}{2}(\nu k^2 + \nu_m k_\perp^2 + \nu_{\text{eff}} k_\parallel^2). \quad (2.72)$$

If neutral atoms are present, the damping is primarily accounted for by the high effective collisional viscosity. This takes place for $k_\parallel^2/k_\perp^2 \gg \nu_m/\nu_{\text{eff}}$. In the absence of the neutral component ($\nu_m = \nu_{\text{eff}}$) we obtain standard expression $\gamma_A = (\nu + \nu_m)k^2/2$.

Magnetosonic Waves For simplicity we suppose $c_s^2 \ll v_A^2$, omit the kinematic viscosity and the heat conductivity, while take into account the magnetic diffusivity, which yields

$$\gamma_f = \frac{1}{2}\nu_{\text{eff}}k^2, \quad \gamma_{\text{slow}} = \frac{c_s^2}{2v_A^2}\nu_{\text{eff}}k_\perp^2. \quad (2.73)$$

If $k_\perp \rightarrow 0$, expression (2.73) gives $\gamma_{\text{slow}} \rightarrow 0$ in this approximations. In fact, the slow magnetosonic wave converts here to the usual sound wave and so damping rate Eq. (2.71) applies.

2.5 Solar and Stellar Winds

Plasma motions allowing the MHD description are highly typical for the astrophysics context. Many objects (typically, those with fast rotation) form accretion disks and produce collimated flows of the plasma—astrophysical jets; others produce more isotropic winds. We emphasize that both these kinds of the plasma outflows are very common. The jets are observed or implied in galactic microquasars, in active galactic nuclei, quasars, blazars, and gamma-ray burst sources; see Sect. 12.4. In many cases the plasma moves with relativistic or even ultrarelativistic speed in these jets.

More isotropic winds are typical for galaxies and normal stars (e.g., Fig. 1.3), although neutron stars produce ultrarelativistic “pulsar winds” in some cases, resulting in a phenomenon of pulsar wind nebulae (e.g., Figs. 1.6 and 1.7 and Sect. 12.3). As a simpler example, we consider here nonrelativistic winds of the normal stars.

The idea of stellar/solar wind had been around well before the space era; however, it was not clear if the corpuscular flows from stars are sporadic or persistent. Direct measurement of the persistent corpuscular flow from the Sun was performed in Greenhouse’s experiment on board Sputnik “Luna-2” in 1959 and then confirmed by satellite Mariner-2 measurements. Soon after this fundamental discovery, the stellar winds were detected (indirectly) from stars of spectral types O and B during the 1960s of the twentieth century. It was established that many (most of the) hot massive ($M \gtrsim 10M_\odot$) high-luminosity stars produce their winds with a very large mass loss rate (Lozinskaya 1992). For example, for the Wolf–Rayet (WR) and Of stars the

mass loss rate is about $\dot{M} \approx (10^{-5} - 10^{-4}) M_{\odot}/\text{year}$; thus, the star can lose a considerable fraction of its mass over time of the order of 10^6 years that is very modest time compared with other astronomic timescales. For example, the Earth are known to exist about 4.5×10^9 years, while the Sun has been shining even longer. The stellar wind speeds were found to range within $u \approx (1 - 4) \times 10^3 \text{ km/s}$. This implies a major deposition of the wind energy into the interstellar medium: with the above values one can easily estimate that the stellar wind energy deposition over the star lifetime, $\sim 10^6$ years, is around $(0.1 - 10) \times 10^{51} \text{ erg}$, which is comparable with the energy released during the supernova explosion occurring at the end of the massive star evolution.

Thus, the stellar wind is not a minor effect; rather it can have numerous dynamical and evolutionary implications. For example, the rapid mass loss, $(10^{-5} - 10^{-6}) M_{\odot}/\text{year}$, affects the star evolution itself including the end of its evolution—supernova explosion, and the supernova remnant expansion—which occurs in a “preprocessed” circumstellar cavity filled by the stellar wind rather than in an average interstellar medium. That strong stellar winds affect the interstellar medium by the deposition of energy and chemical elements and disturbing its dynamics parameters, including the ISM magnetic field. Given that the massive stars are not randomly distributed in the Galaxy, but correlated within so-called OB associations, the stellar winds from different stars can interact with each other and merge into a powerful velocity field additionally enhanced by supernova explosions within the association. These interacting winds form a bubble (also called “superbubble”) with a linear scale up to a few hundred pc, which is bounded by a cooler supershell expanding as a single object due to cumulative pressure produced by the winds and explosions. We will be returning to these phenomena below in the book.

Although hundreds of stars with high luminosity L within $(5 \times 10^2 - 5 \times 10^7) L_{\odot}$ were observed to produce the winds with the mass rate within $\dot{M} \approx 10^{-9} M_{\odot}/\text{year}$ and $\dot{M} \approx 10^{-4} M_{\odot}/\text{year}$, the mass losses in the form of the wind are also typical for stars with much weaker luminosity. For example, observations favor winds from much less luminous stars, e.g., cool massive red giants ($\dot{M} \approx 10^{-6} M_{\odot}/\text{year}$, $u \approx 10 \text{ km/s}$), from nuclei of planetary nebulae with the speed $(2 - 3) \times 10^3 \text{ km/s}$ (which is 3–4 times larger than the gravitation runaway velocity) and the mass loss rate $\dot{M} \approx (4 \times 10^{-9} - 7 \times 10^{-7}) M_{\odot}/\text{year}$, and, finally, from the closest to the Earth star, the Sun.

2.5.1 Basic Observational Data About the Solar Wind

The solar wind is one of the main constituents which, along with eruptive phenomena and electromagnetic radiation from the Sun and planets, determines physical conditions in the circumsolar space (Fig. 1.3). The solar wind is a more or less stationary and isotropic plasma flow, which is launched in the upper corona of the Sun and transfers magnetic fields of solar origin. The first

indications of some corpuscular flow outward the Sun in interplanetary space were obtained in the nineteenth century (e.g., see Brandt 1970 for a review). The persistent character of the solar wind was experimentally established by Biermann (1951, 1952) via investigation of the behavior of comet tails. This result was further confirmed indirectly by observations of modulation of the galactic cosmic rays and by data on geomagnetic activity and auroras.

Direct measurements of the interplanetary plasma parameters became possible in the space era by Earth-orbiting satellites and also by interplanetary spacecraft missions. They provide quasi-continuous measurements of the interplanetary plasma physical parameters in various locations of the space. Remarkably, the parameters of the solar wind, the particle number density, abundances, velocity, and temperature experience significant temporal and spatial variations. Nowadays, the running combination of the involved IPM parameters and their drivers are collectively called the “space weather” (Gary and Keller 2004).

The measurements at the Earth orbit give the solar wind velocity (mass velocity) u between ≈ 300 and ≈ 700 km/s (the mean value is ≈ 400 km/s; the highest values of $\approx 2,000$ km/s are measured in association with sequences of largest solar flares, e.g., in November 2003); the ion number density $\approx 5 \text{ cm}^{-3}$; the flux density of positive ions $2 \times 10^8 \text{ cm}^{-2} \text{ s}^{-1}$ and the temperature $T_p \approx 3 \times 10^4 - 6 \times 10^5 \text{ K}$ (the mean value is $1.5 \times 10^5 \text{ K}$) for protons and $T_e \approx 1.5 \times 10^5$ for electrons. The number density of He^{++} ions (the α -particles) is usually around 4–5 % of the proton number density. The number of neutral atoms is insignificant. The magnetic field is measured to be highly variable and typically to belong the range $(1-10) \times 10^{-5} \text{ G}$ with the mean value of $B \approx 5 \times 10^{-5} \text{ G}$. Solar wind is a supersonic flow, whose Mach numbers $M = u/v_{Ti}$ and $M_A = u/v_A$ have values 8–10.

The numbers allow estimating typical values of the solar wind kinetic energy density $n_i m_i u^2 / 2 \approx 10^{-9} \text{ erg cm}^{-3}$ and the magnetic energy density $B^2 / 8\pi \approx 10^{-10} \text{ erg cm}^{-3}$ near the Earth orbit, so the kinetic energy of the hydrodynamic flow exceeds the magnetic energy by a factor of ten. This allows neglecting the electromagnetic forces and considering the solar wind as a purely hydrodynamic flow to the first approximation. But before applying the HD we have to check if condition (2.9) $\Lambda_{ii} \ll r$ is fulfilled, where r is heliocentric distance and Λ_{ii} is the ion mean free path. We have $\Lambda_{ii} = 1/n_i \sigma_{ii}$ and use the Coulomb cross section $\sigma_{ii} \approx \pi(e^2/m_i v_{Ti}^2)^2 \ln \Lambda_C \approx \pi(e^2/T_i)^2 \ln \Lambda_C$ obtained for the thermal plasma (see Sect. 1.3.7). It is then convenient to express the mean free path Λ_{ii} in astronomical units ($1 \text{ AU} \approx 1.49 \times 10^{13} \text{ cm}$):

$$\Lambda_{ii} \approx 0.7 \times 10^{-9} T_i^2 / n_i, \quad (2.74)$$

where the temperature and the number density are in Kelvin and cm^{-3} , respectively.

Adopting the coronal values $n_i = 2 \times 10^8 \text{ cm}^{-3}$ and $T_i = 2 \times 10^6 \text{ K}$ for the height at which the solar wind is launched, we obtain $\Lambda_{ii} \approx 2 \times 10^8 \text{ cm}$

$\ll R_\odot \approx 7 \times 10^{10}$ cm; thus, the hydrodynamic description is applicable here. However, at the Earth orbit, we have $T_i \approx 10^5$ K and $n_i \approx 5 \text{ cm}^{-3}$. Formula (2.74) gives $\Lambda_{ii} \approx 1$ AU in this case, i.e., $\Lambda_{ii} \approx r$, so the space plasma is collisionless and the hydrodynamic approach seems to fail. Nevertheless, as we have discussed in Sect. 1.3.8, the anomalous processes can strongly reduce the particle mean free path in the collisionless plasma compared with that determined by the Coulomb scattering only. Fluctuations of interplanetary magnetic field and plasma waves developed due to different plasma instabilities make the particle trajectories tangled and the velocities more isotropic, and so reduce their mean free paths, which ensures broader applicability of the HD/MHD approach than it could be anticipated. Complementary, the effective mean free path of solar wind protons was measured from experimental data about its distribution function (see, e.g., the first data reported by Brandt et al. 1973; Marsch et al. 1982a,b). The anomalous mean free path varies depending on the IPM state and was found to be well below 0.1 AU in many cases. This remarkable finding justifies approximate applicability of the standard HD equations to describe the solar wind at 1 AU and farther away from the Sun.

It should be emphasized, however, that for the number densities and temperatures typical for the interplanetary plasma, the mean free path of particles with respect to Coulomb collisions is rather large and often exceeds 1 AU. Thus, the particle distributions are not necessarily isotropic, and particle distribution functions are not necessarily Maxwellian (see Sect. 1.3.8). In agreement with this expectation, the measured steady-state distribution function of the solar wind particles is typically well described by a *kappa* distribution, rather than a Maxwellian. The thermal energies of electrons and ions (i.e., the electron and ion effective temperatures) are often different. This means that the solar wind is seldom (never) in a state of a true thermodynamic equilibrium.

We note that the Sun loses an extremely small part of its mass in the form of the solar wind. The discussed parameters of the solar wind allow estimating the entire mass flow from the Sun: $J_M = 4\pi r_0^2 u m_i n_i \approx 10^{19}$ g/year $\approx 10^{-14} M_\odot$ /year, where $r_0 = 1$ AU, $M_\odot \approx 2 \times 10^{33}$ g is the solar mass. During the Sun lifetime ($< 10^{10}$ years) the solar wind has taken out total of only $10^{-4} M_\odot$ if we adopt that the flow parameters are more or less constant over this time.

2.5.2 Parker's Model of the Solar Corona Expansion

Let us apply, following Parker (1963), the HD equations to understand the phenomenon of the solar wind. We start with analysis of the *hydrostatic* ($\partial/\partial t = 0$ and $\mathbf{u} = 0$) equilibrium of a spherically symmetric fully ionized hydrogen atmosphere to which the equation of state, Eq. (2.23),

$P(r) = 2n_i(r)T(r)$ of a tenuous gas applies. Neglecting electromagnetic forces, Eq.(2.2) requires that the pressure gradient is balanced by the gravitation force:

$$\frac{d}{dr} 2n_i T + \frac{GM_\odot m_i n_i}{r^2} = 0, \quad (2.75)$$

where $G \approx 6.67 \times 10^{-8} \text{ cm}^3 \text{ g}^{-1} \text{ s}^2 = 6.67 \times 10^{-11} \text{ m}^3 \text{ kg}^{-1} \text{ s}^2$ is the gravitational constant. Integration of this equation yields

$$n_i(r)T(r) = n_i(r_0)T(r_0) \exp \left[-\frac{GM_\odot m_i}{2} \int_{r_0}^r \frac{ds}{s^2 T(s)} \right]. \quad (2.76)$$

Remarkable conclusions about the hydrostatic equilibrium can be derived from analysis of the rhs of the equation. Indeed, if the temperature $T(r)$ decreases with r faster than r^{-1} then the exponent index decreases infinitely at $r \rightarrow \infty$ and, thus, $n_i(r)T(r) \rightarrow 0$ at the infinity. Stated another way, this tells us that the stellar atmosphere has a finite size and a hydrostatic equilibrium is achievable.² The only way of the atmosphere dissipation here is gravitation runaway of higher-energy particles from a “tail” of the steady-state distribution, which is beyond the HD applicability region.

However, if the temperature decreases slower than r^{-1} then the exponent index in Eq. (2.76) has a finite value at arbitrarily large r , which implies a finite pressure at the infinity. Since a finite gas amount (stellar atmosphere) cannot be distributed over an infinite volume with a finite density, we arrive at a conclusion that no hydrostatic equilibrium is possible in this case; thus, a HD expansion with some $u(r) \neq 0$ must appear.

Let us consider this expansion assuming the motion to be stationary ($\partial/\partial t = 0$ as before). We use the equation of mass conservation

$$n_i(r)u(r)r^2 = n_i(r_0)u(r_0)r_0^2, \quad (2.77)$$

where r_0 is the stellar radius at the base of corona, and the equation of motion

$$m_i n_i u \frac{du}{dr} + \frac{d}{dr} 2n_i T + \frac{GM_\odot m_i n_i}{r^2} = 0. \quad (2.78)$$

Full solution of the problem requires also an energy transfer equation. However, the fundamental science question of the mechanisms of the solar wind heating (and, more generally, of the corona heating) is highly sophisticated and has not yet been fully understood, which will be discussed in greater detail later. Now, to make a qualitative progress, we adopt a simple power law for the temperature dependence on r without assuming a specific mechanism of the corona heating.

²It must be noted that such hydrostatic equilibrium is not necessarily stable: for example, it can be convectively unstable if the temperature gradient is large; see Chap. 6.

It is convenient to introduce two characteristic proton velocities, the thermal speed (which is also the “isothermal” speed of sound)

$$v_T(r) = [2T(r)/m_i]^{1/2} \quad (2.79)$$

and the runaway velocity from r_0

$$v_e = (GM_\odot/r_0)^{1/2} = \text{const.} \quad (2.80)$$

With this notations Eq. (2.78) receives the form

$$u \frac{du}{dr} \left(1 - \frac{v_T^2}{u^2} \right) = R(r), \quad (2.81)$$

where

$$R(r) = -r^2 \frac{d}{dr} \frac{v_T^2}{r^2} - \frac{v_e^2 r_0}{r^2}. \quad (2.82)$$

We consider the case when the atmosphere is strongly coupled with the star $v_e^2 \gg v_T^2(r_0) \gg u^2(r_0)$ at the level $r = r_0$, while the temperature T monotonously decreases with r slower than r^{-1} , i.e., $T(r) = T_0(r/r_0)^{\varepsilon-1}$, $0 < \varepsilon < 1$, $T(\infty) \rightarrow 0$. For $r \rightarrow r_0$ we have $R(r) < 0$ because $v_e^2 \gg v_T^2$. Nevertheless, the first term in the rhs of Eq. (2.82) is positive and decreases slower than r^{-2} . Therefore, a “critical layer” $r = r_c$ exists, where $R(r_c) = 0$, with $R(r) > 0$ at $r > r_c$ and $R(r) < 0$ at $r < r_c$. Since at the corona base, $r = r_0$, the expansion is weak, $u^2 \ll v_T^2$, then both values entering Eq. (2.81), $1 - v_T^2/u^2$ and $R(r)$, are negative, so $du/dr > 0$ is positive, i.e., the gas is being accelerated by the pressure gradient.

Consider what can happen to the flow farther away from the star. If, (1) during the gas acceleration, the flow velocity u reaches the value of v_T somewhere at $r < r_c$ then $du/dr \rightarrow \infty$ at $v_T = u$ according to Eq. (2.81), while the flow velocity is directed toward the star at larger r (see curve 1 in Fig. 2.2). Such solutions seem to be inconsistent with the adopted stationarity of the flow and so require account of the time derivative in Eq. (2.2). If (2) the equality $v_T = u$ is not achieved at $r < r_c$, then the derivative du/dr becomes negative at $r > r_c$, and the gas motion remains subsonic at the entire space decaying gradually at large distance from the star. Such solutions (see curve 2 in Fig. 2.2) are called the *stellar breeze* to distinguish from supersonic solar *wind*. Finally, (3) if the expansion velocity u reaches the thermal velocity v_T at the very same layer r_c , where $R(r_c) = 0$ (curve 3 in Fig. 2.2), then the stellar wind becomes supersonic at $r > r_c$, where it keeps accelerating. This solution does correspond (qualitatively) to the solar wind actually observed in the IPM. For any given temperature profile, one can plot dependences of u and other relevant parameters on r numerically.

We must emphasize, however, that even though the model considered uncovers the fundamentals behind the solar wind phenomenon, it remains

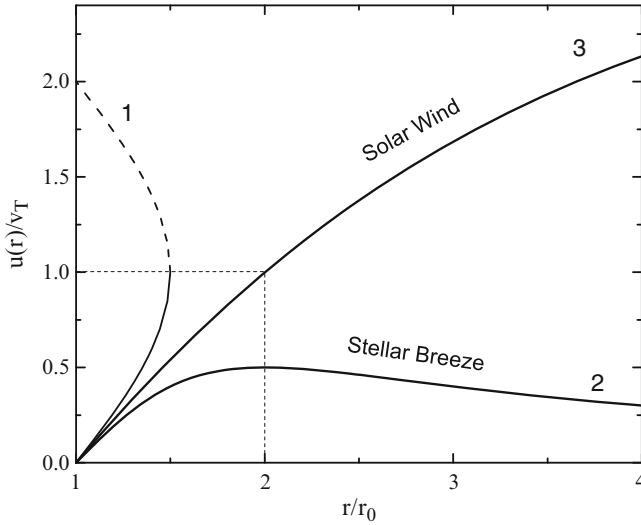


Figure 2.2: Solutions for the plasma outflow from a star: (1) double valued and so unphysical flow; (2) subsonic stellar breeze; and (3) supersonic stellar wind. In this example the critical radius $r_c = 2r_0$.

highly idealized and incomplete. In particular, it ignores the magnetic field, the star rotation, the difference between electron and ion temperatures, departure from the thermodynamic equilibrium, all kinds of inhomogeneity, nonstationarity, and heating mechanisms, all of which can have major effect on the solar wind properties. For example, eruptive processes in the solar corona often give rise to ejections of large massive plasma clouds (so-called coronal mass ejections, CMEs), which have huge effect on the space weather at the Earth orbit.

A fundamental question of an additional plasma heating, which is vital for the solar wind phenomenon, deserves more discussion. We have already noticed that to allow for the solar wind acceleration, the plasma temperature must not decrease too rapidly with r . In fact, as we are going to show below, an additional energy deposition is critically needed for the gas to overcome the gravitation force and acquire a supersonic speed.

To make this clear we note that according to Eq. (2.77) the density of expanding plasma obeys the law:

$$n_i(r) = n_i(r_0) \frac{u(r_0)r_0^2}{u(r)r^2}. \quad (2.83)$$

If no energy deposition is present, the gas expands adiabatically:

$$T = T_0(n_i/n_{i0})^{\gamma-1}, \quad (2.84)$$

with the ratio of specific heats $\gamma = 5/3$ for a single-atom gas. Thus, the

temperature decreases as

$$T \sim u^{-(\gamma-1)} r^{-2(\gamma-1)}, \quad (2.85)$$

i.e., $\propto r^{-4/3}$ for a constant expansion velocity and even faster for an accelerated expansion, which is in all the cases faster than a limiting temperature profile $\propto r^{-1}$ obtained from Eq. (2.76).

Let us estimate the required heat deposition based on the energy balance consideration (Parker 1979). The gravitation energy density per unit volume is

$$\Phi(r) = -\frac{GM_{\odot}m_i n_i}{r}. \quad (2.86)$$

The energy, which is spent for the gas to overcome the gravitation field and to accelerate the gas, is the enthalpy, which accounts the work of the pressure force:

$$w = \epsilon + P = \frac{2\gamma}{\gamma-1} n_i T. \quad (2.87)$$

Here $\epsilon = n_i T / (\gamma - 1)$ is the internal energy density. The ratio

$$\frac{w}{|\Phi(r_0)|} = \frac{5T r_0}{GM_{\odot} m_i} \approx 0.43 \quad (2.88)$$

is less than one for $r = r_0 \approx 0.7 \times 10^{11}$ cm and $T \approx 2 \times 10^6$ K and so is insufficient to produce the wind. Therefore, to overcome the gravitation and to accelerate then gas up to 400 km/s an additional energy Q must indeed be deposited. In place of explicit account of the energy sources, we describe this energy deposition by using the polytropic equation instead the adiabatic one:

$$T = T_0 (n_i / n_{0i})^{\alpha-1}, \quad (2.89)$$

where α is the polytropic index. For $\alpha < \gamma$ comparison of Eq. (2.89) with adiabatic equation (2.84) reveals that for the same gas expansion n_i / n_{0i} , the temperature is larger for polytropic process than for the adiabatic process. Therefore, this does account for an additional heat deposition into the gas, with the heat efficiency defined by the polytropic index; apparently, no information on the physical mechanisms of the plasma heating is available in Eq. (2.89) within this treatment.

We can now introduce an effective enthalpy w_{eff} accounting for the additional heat deposition in the form of Eq. (2.87) with the polytropic index α in place of the adiabatic index: γ

$$w_{\text{eff}} = \frac{2\alpha}{\alpha-1} n_i T. \quad (2.90)$$

The required polytropic index then can easily be estimated from the energy conservation per particle at the corona base and far away from the Sun in a region of the supersonic wind:

$$\frac{2\alpha}{\alpha - 1}T_0 - \frac{GM_\odot m_i n_i}{r_0} = \frac{m_i u^2(r)}{2}. \quad (2.91)$$

Here we neglected the expansion velocity at the corona base and neglected thermal energy and gravitation potential far away from the Sun. Substitution of the mean solar wind speed $u(r) = 400$ km/s and typical coronal parameters yields $\alpha \approx 1.14$; Parker (1979) proposed $1.0 < \alpha < 1.3$ as the most plausible range for the polytropic indices. Equation (2.91) also tells us that for low coronal temperature

$$T_0 < \frac{(\alpha - 1)Gm_i M_\odot}{2\alpha r_0}, \quad (2.92)$$

the expansion is impossible and the corona remains static.

Let us touch upon possible mechanisms of the additional heat deposition into the expanding plasma. Generally, there are absorption of the solar radiation flux, standard heat conductivity, losses of nonthermal particle population, and dissipation of various plasma/MHD waves, which are efficiently generated in the convective zone of the Sun and then transferred outward to the corona. First three mechanisms are easy to take into account; it turns that all they are insufficient to provide the required plasma heating. We, therefore, forced to conclude that the primary source of the heat is the wave dissipation. However, it is extremely difficult to quantitatively check this conclusion because the theory of wave generation, propagation, and damping is very complicated and in addition depends on poorly known details of the solar atmosphere structure and relevant physical conditions. We will consider some of the related processes and phenomena below in this book; however, the current state of the science is yet unable to fully describe the phenomenon of the solar wind and in particular—reliably identify the sources and mechanisms of the additional corona heating.

The discussed simplest model of the uniform corona expansion suggests that the solar wind overcomes the sound speed and becomes supersonic at around $r_c \approx 10r_\odot$. Accordingly, at the Earth orbit, the plasma flow is highly supersonic and supersonic. We note that a very interesting physics takes place at those regions where such a supersonic flow interacts with an obstacle. A practically important and actively studied example of this is the interaction of the solar wind with the Earth's magnetosphere (Fig. 1.3), which results in a variety of observable manifestations including the polar lights (Fig. 1.4).

Then, as the wind propagates farther away from the Sun, the ISM surrounding the solar system starts to affect and modify the solar wind (see, e.g., Hundhausen 1972; Baranov and Krasnobaev 1977). Indeed, if the interstellar medium pressure were absent, the solar wind speed would remain

approximately constant, of the order of 400 km s^{-1} ; its number density would fall with distance as r^{-2} , and the temperature would also decrease as described. Hence, the solar wind would become more and more supersonic. However, in the real situation, the solar wind is slowed down by the interstellar medium and, therefore, the supersonic regime should give a way to a subsonic one at some distance from the Sun, which is accompanied by the appearance of a termination shock.

A rough estimate of the shock position r_{sh} may be obtained from the requirement of balance between the solar wind dynamic pressure and interstellar medium pressure:

$$n_i m_i u^2 \approx (n_a + 2n_e)T + \frac{B^2}{8\pi} + P_{\text{CR}}, \quad (2.93)$$

where P_{CR} is the cosmic ray (relativistic particles) pressure, n_a is the number density of neutral atoms in interstellar medium, n_e is the electron number density in interstellar medium, and T is its temperature. Substituting $n_i = n_{iE} r^{-2}$, where $n_{iE} \approx 5 \text{ cm}^{-3}$ and r_{Tsh} is the distance in AU, and other parameters adopted above, we obtain $r_{Tsh} \approx 100 \text{ AU}$.

A number of space missions have been launched toward the anticipated bounds of the solar system years ago to determine where those bounds are and what are the physical conditions there. The first reliable detection of the termination shock occurred on December 14, 2004, by a spacecraft Voyager 1 at the distance 94 AU from the Sun. It took around 30 years for the spacecraft, launched on 1977, to path through the solar system. Later, Voyager 2 having a different trajectory detected the termination shock at the distance 84 AU on August 30, 2007. In fact, Voyager 2 detected the termination shock a few times: this is because the position of the termination shock is changing in time in response to short-term variations of the solar activity. It is supposed that the shock position also experiences systematic changes back and forth following the 11 years cycle of the solar activity. According to the measurements made by Voyagers 1 and 2, the solar wind velocity near the heliospheric shock wave was approximately 380 km/s , and the ratio $u_1/u_2 = \rho_2/\rho_1 \approx 3$ at the front.

2.5.3 Magnetic Field in a Cavity Filled by a Stellar Wind

Consider now another important constituent of the solar wind, the mean magnetic field. Specifically, let us apply dissipation-free induction equations (2.33) to calculate the magnetic field structure in a volume filled by solar or stellar wind within a simple model. Here, we adopt that the plasma is launched isotropically from a spherical surface of the radius a , rotating around a central axes with constant angular velocity Ω . The stellar wind speed u is constant and has radial direction. At the spherical surface there is a magnetic field,

which is described by the function $\mathbf{B}(a, \vartheta, \alpha) = \mathbf{B}_0(\vartheta, \alpha)$ in the reference frame rotating together with the star, where α is the azimuth angle in the plane transverse to the rotation axes. The energy density of the plasma motion exceeds significantly the energy density of the magnetic field; thus, we can neglect the magnetic field effect on the plasma motion. Using the freezing-in condition we find here the magnetic field distribution (dependence of the magnetic field on the coordinates and time) in the region $r > a$ in the laboratory (rest frame) system.³

To solve this problem we first project vector equation (2.38) to the axes r and substitute $\mathbf{u} = u\mathbf{r}/r$, $u = \text{const}$, which yields the equation for B_r :

$$\frac{\partial B_r}{\partial t} = -\frac{2u}{r}B_r - u\frac{\partial B_r}{\partial r}. \quad (2.94)$$

Solution of this equation is an arbitrary function of independent variables $r - ut$, ϑ , and α divided by r^2 :

$$B_r(r, \vartheta, \alpha, t) = \frac{1}{r^2}F(r - ut, \vartheta, \alpha). \quad (2.95)$$

The boundary condition has evidently the form

$$B_r|_{r=a} = B_{0r}(\vartheta, \alpha + \Omega t) = \frac{1}{a^2}F(a - ut, \vartheta, \alpha), \quad (2.96)$$

where the argument $\alpha + \Omega t$ in B_{0r} originates from the transition from the rotating frame to the laboratory rest frame; therefore

$$F(a - ut, \vartheta, \alpha) = a^2 B_{0r}(\vartheta, \alpha + \Omega t)$$

and solution (2.95) reads

$$B_r(r, \vartheta, \alpha, t) = \left(\frac{a}{r}\right)^2 B_{0r}\left(\vartheta, \alpha - \frac{(r-a)\Omega}{u} + \Omega t\right). \quad (2.97)$$

In a similar way, we find two remaining components of the magnetic field:

$$B_\vartheta = \frac{a}{r}B_{0\vartheta}\left(\vartheta, \alpha - \frac{(r-a)\Omega}{u} + \Omega t\right), \quad (2.98a)$$

$$B_\alpha = \frac{a}{r}B_{0\alpha}\left(\vartheta, \alpha - \frac{(r-a)\Omega}{u} + \Omega t\right). \quad (2.98b)$$

³The model considered here was proposed by Parker (1959) to describe the interplanetary magnetic field produced by the solar plasma flows composing the solar wind.

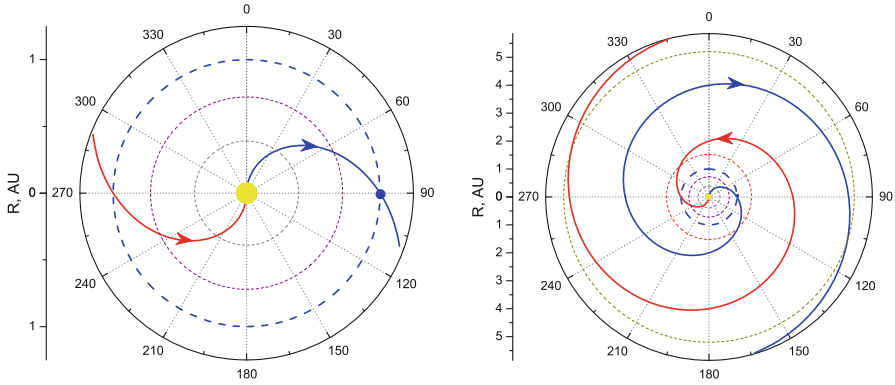


Figure 2.3: Two oppositely directed magnetic field lines illustrating the Parker model of the IPM magnetic field at the scale of the Earth (*left*) and Jupiter (*right*) orbits. The planet orbits are shown by *dashed color circles* (the orbit eccentricities are neglected) for Mercury (*grey*), Venus (*violet*), Earth (*bold blue*); the planet itself is shown by *blue circle*; not in scale), Mars (*red*), and Jupiter (*brown*).

Using Maxwell equation $\nabla \cdot \mathbf{B} = 0$ and Eq. (2.97) gives rise to the following useful relationship between components of the vector \mathbf{B}_0 :

$$-\frac{a\Omega}{u} \frac{\partial B_{0r}}{\partial \alpha} \sin \vartheta + \frac{\partial}{\partial \vartheta} (B_{0\vartheta} \sin \vartheta) + \frac{\partial B_{0\alpha}}{\partial \alpha} = 0.$$

For example, if $B_{0\vartheta} = 0$ then $B_{\vartheta} = 0$ during the entire field evolution, and

$$B_{0\alpha} = \frac{a\Omega}{u} B_{0r} \sin \vartheta + f(\vartheta).$$

If we further adopt $f(\vartheta) = 0$, we then obtain

$$B_{\alpha}(r, \vartheta, \alpha, t) = \frac{a^2 \Omega}{ur} B_{0r} \left(\vartheta, \alpha - \frac{(r-a)\Omega}{u} + \Omega t \right) \sin \vartheta. \quad (2.99)$$

Equations (2.97) and (2.99) show that the azimuth component of the magnetic field decreases with r much slower, as $\propto r^{-1}$, than the radial component does, as $\propto r^{-2}$. Thus, even if the radial component of the magnetic field dominates at the star surface, the azimuth component dominates farther away from the star, which gives rise to the spiral shape of the mean interplanetary magnetic field.

Parker applied this model to describe the interplanetary magnetic field of the solar wind (Fig. 2.3). The original Parker's model adopts $B_{\vartheta} = 0$, while B_r and B_{α} are described by Eqs. (2.97) and (2.99). Measurements of the interplanetary magnetic field indicate the presence of a slowly varying

component, which indeed has an approximately spiral structure and intersects the Earth orbit at an angle of 45° . The average magnetic field near the Earth orbit is close to 5×10^{-5} G, though the measured values are scattered very strongly. At low heliographic latitudes the spiral field consists of several sectors with mutually opposite magnetic field directions. The radial component varies with distance as r^{-2} , in good agreement with the Parker model. However, the agreement is much poorer for the azimuthal component, which displays the dependences from $B_\alpha \sim r^{-1.23}$ to $\sim r^{-1.1}$ between 1 and 5 AU. The component $B_\theta < 10^{-5}$ G was also observed near the Earth orbit.

The magnetic field structure unlike the solar wind itself is not spherically symmetric. Given that the magnetic energy density is one–two orders of magnitude smaller than the kinetic energy of the solar wind, thus, a relatively weak deviation of the solar wind from the spherically symmetric flow can have major effect on the magnetic field structure. Even though observations do often reveal significant departure of the measured magnetic field from the Parker's one, the overall agreement is, nevertheless, remarkably good especially if one takes into account the number of the simplifications adopted.

Problems

2.1 Using the Faraday induction law and dissipation-free equations (2.28), prove that the magnetic flux through arbitrary closed contour remains constant regardless contour motions and deformations.

2.2 Adopt stationary equilibrium of the conducting fluid in a magnetic field. Demonstrate that the vectors of the magnetic field \mathbf{B} and the current density \mathbf{j} are tangent to the surfaces $p(\mathbf{r}) = \text{const}$.

2.3 Adopt that electric current J flows along a hot plasma cylinder with radius a and a nonuniform current density $j(r)$ (z -pinch). Find stationary solution $P(r)$ for the plasma pressure under the condition that this pressure is compensated by the magnetic pressure produced by this electric current itself. Write down a relation linking the total electric current of the pinch and the pinch pressure integrated over pinch cross section.

Adopt then that the plasma is isothermal and obeys the ideal gas equation of state [Eq. (2.23)]. Express current J via the plasma temperature T and the total number of the plasma electrons (or ions) N per unit length of the cylinder. Calculate the current assuming $N \approx 10^{15}$ ions/cm and $T \approx 10^8$ K—the parameters typical for the nuclear fusion studies; see Fig. 1.1.

2.4 Determine equilibrium condition for the plasma cylinder with radius a , in which the electric current has only azimuth component $j_\alpha(r)$ (so-called theta pinch). The outside pressure is small and can be discarded compared with the pinch pressure. Is it possible to ensure equilibrium using some distribution of the magnetic field produced by external sources?

2.5 The magnetic field is called the *force-free field* (Sect. 2.3.3) if the density of Ampère's force is zero everywhere: $\mathbf{j} \times \mathbf{B}/c = 0$. To ensure this, it is apparently necessary and sufficient that the electric current is directed along the field lines everywhere.

- (a) Show that the force-free field \mathbf{B} satisfies the equation set:

$$\nabla \times \mathbf{B} = \alpha_{FFF} \mathbf{B}, \quad \mathbf{B} \cdot \nabla \alpha_{FFF} = 0,$$

where $\alpha_{FFF}(\mathbf{r})$ is arbitrary differentiable scalar function (including constant).

- (b) Derive a force-free field dependent on r only in cylindrical coordinates for $\alpha_{FFF} = \text{const}$.
- (c) Is it possible to have a finite energy of the force-free field for $\alpha_{FFF} = \text{const}$?
- (d) Prove that $\alpha_{FFF} = \text{const}$ for any force-free field along any field line.

2.6 Consider modification of MHD eigenmodes in a plasma permitted by a nonpotential force-free magnetic field and calculate the corresponding kinetic helicity density defined as $h_k = \langle \mathbf{u}(\mathbf{r}, t) \cdot \nabla \times \mathbf{u}(\mathbf{r}, t) \rangle$.

2.7 Adopt that a stationary velocity field $\mathbf{u} = (u_x(y, z), 0, 0)$ holds in a conducting fluid (shear motion). The initial condition at $t = 0$ for the magnetic field is $\mathbf{B}_0 = (0, B_{0y}(y, z), B_{0z}(y, z))$. Apply dissipation-free approximation ($\nu_m \rightarrow \infty$) to derive the field at $t > 0$.

2.8 A stationary differential rotation (i.e., various fluid layer rotate with different velocities) with an angular velocity $\Omega = \mathbf{e}_z \Omega(r, \vartheta)$, where r, ϑ are the spherical coordinates, holds in a conducting fluid. Originally, the magnetic field is poloidal, i.e., it belongs to meridian planes: at $t = 0$, $\mathbf{B} = (B_{0r}(r, \vartheta), B_{0\vartheta}(r, \vartheta), 0)$. Calculate the magnetic field at $t > 0$ neglecting the dissipation in the plasma.

2.9 Derive equation (2.98).

2.10 Plot dependences of u and other relevant parameters of the Parker's stellar wind on r numerically for different temperature profiles.

2.11 Find the form of interplanetary magnetic field force lines in Parker's model (see Sect. 2.5.3). Calculate magnetic field value and the angle θ between force line and radial direction at the Earth orbit. The solar radius is $a = 0.7 \times 10^6$ km; the mean magnetic field at the solar surface $B_0 \approx 1$ G; the radius of Earth orbit $r_0 \approx 1.5 \times 10^8$ km; the angular velocity of solar rotation $\Omega = 2.7 \times 10^{-6}$ rad/s; solar wind velocity $u = 300$ km/s (slow solar wind).

2.12 Demonstrate that the solution for the magnetic field in stationary radial stellar wind (see Sect. 2.5.3) has the form

$$\begin{aligned} B_r(r, \vartheta, \alpha, t) &= F \left(\alpha - \frac{(r-a)\Omega}{u} + \Omega t \right) \left(\frac{a}{r} \right)^2 2 \cos \vartheta, \\ B_\vartheta(r, \vartheta, \alpha, t) &= p \frac{\partial}{\partial \alpha} F \left(\alpha - \frac{(r-a)\Omega}{u} + \Omega t \right) \frac{a^2 \Omega}{ur} \sin \vartheta, \\ B_\alpha(r, \vartheta, \alpha, t) &= q F \left(\alpha - \frac{(r-a)\Omega}{u} + \Omega t \right) \frac{a^2 \Omega}{ur} 2 \sin \vartheta \cos \vartheta. \end{aligned}$$

Here p and q are constants, which satisfy the condition $p+q=1$, and F is an arbitrary function, specified by the boundary conditions at the solar surface.

Answers and Solutions

2.2 In the static equilibrium ($\mathbf{u} = 0$) and in the absence of non-electromagnetic forces the equilibrium condition reads $\nabla p = \mathbf{j} \times \mathbf{B}/c$. Thus the vectors \mathbf{B} and \mathbf{j} are transverse to the pressure gradient and so tangent to the isobaric surfaces.

2.3 The magnetic field has one component:

$$B_\varphi \equiv B(r) = \frac{4\pi}{cr} \int_0^r r j(r) dr.$$

Integrating the equilibrium condition, which follows from Eq. (2.13a) for $u=0$ with the boundary condition $p|_{r=a} = 0$, we obtain

$$p(r) = \frac{1}{8\pi} \int_r^a \frac{1}{r^2} \frac{d}{dr} (r^2 B^2) dr, \quad (1)$$

where $B = (4\pi/cr) \int_0^r r j(r) dr$ at $r < a$ and $B = 2J/cr$ at $r > a$. To link the total current with the pressure we integrate Eq. (1) over full transverse section and apply the relation $aB(a) = 2J/c$, which yields

$$\int_0^a p(r) 2\pi r dr = \frac{J^2}{2c^2}. \quad (2)$$

Assuming that the plasma is an equilibrium ideal gas with a given temperature T (in units of energy), we adopt $p = 2n(r)T$ and then Eq. (2) yields

$$J = 2c\sqrt{NT}. \quad (3)$$

Substitution of required numbers into (3) results in $J = 7.5 \times 10^4$ A. In practice the plasma is often non-isothermal, with the electron temperature exceeding the ion temperature. To maintain the equilibrium the current must grow in time, because the current results in the increase of both temperature and pressure. In addition, the pinch can become unstable relative to kink or sausage mode instabilities.

2.4 The magnetic field inside the cylinder has one component $B_z(r) \equiv B(r) = (4\pi/c) \int_r^a j_\varphi(r) dr$. The equilibrium inside the cylinder requires constancy of the full pressure:

$$p(r) + \frac{B^2(r)}{8\pi} = \text{const.}$$

Outside the cylinder without any medium we have $p = 0$ and the magnetic field generated by the azimuth current is zero, $B = 0$; thus, the internal pressure can only be balanced by a magnetic pressure produced by a field directed along the cylinder axes, whose value at the side surface of the cylinder is $B_0 = \sqrt{8\pi p(a)}$. The magnetic field inside the cylinder is always smaller than the external field:

$$\frac{B^2}{8\pi} = \frac{B_0^2}{8\pi} - p;$$

thus, the plasma is a diamagnetic.

2.5 (b) $\mathbf{B}(\mathbf{r}) = B_0 \cdot (0, J_1(\alpha_{FFF} r), J_0(\alpha_{FFF} r))$, where $J_n(x)$ is the Bessel function.

2.6 To investigate properties of weakly damping linear modes we neglect the dissipative terms entirely in MHD Eqs. (2.13) and (2.16). Then, for simplicity, we only consider the helicity originating from the magnetic field twist (the corresponding pseudoscalar is formed by the dot product of the polar vector \mathbf{j} and the axial vector \mathbf{B} : $\mathbf{j} \cdot \mathbf{B}$, while no other polar vectors are explicitly considered) and so we neglect the kinetic pressure and the external force assuming that their contribution to the helicity is smaller; so the equations read

$$\nabla \cdot \mathbf{B} = 0, \quad \frac{\partial \mathbf{B}}{\partial t} = \nabla \times [\mathbf{u} \times \mathbf{B}], \quad (2.100a)$$

$$\rho \left(\frac{\partial \mathbf{u}}{\partial t} + (\mathbf{u} \cdot \nabla) \mathbf{u} \right) = \frac{1}{4\pi} [\nabla \times \mathbf{B}] \times \mathbf{B}. \quad (2.100b)$$

Now, to describe the small-amplitude linear modes satisfying these equations, we have to linearize them adopting $\mathbf{B} = \mathbf{B}_0 + \mathbf{b}$ for the magnetic field and adopting \mathbf{b} and \mathbf{u} to be the first-order oscillating values of an MHD mode. Importantly, that upon substitution of $\mathbf{B} = \mathbf{B}_0 + \mathbf{b}$ into Eq. (2.100b) we have to take into account that in the nonpotential force-free field $\nabla \times \mathbf{B}_0 = \alpha_{FFF} \mathbf{B}_0 \neq 0$ unlike cases of a uniform field or nonuniform potential field, which yields

$$\frac{\partial \mathbf{b}}{\partial t} = (\mathbf{B}_0 \cdot \nabla) \mathbf{u} - (\mathbf{u} \cdot \nabla) \mathbf{B}_0, \quad \frac{\partial \mathbf{u}}{\partial t} = \frac{\alpha_{FFF}}{4\pi\rho} \mathbf{B}_0 \times \mathbf{b} + \frac{1}{4\pi\rho} (\nabla \times \mathbf{b}) \times \mathbf{B}_0. \quad (2.101)$$

Within the eikonal approximation (i.e., adopting the wavelengths of the eigenmodes to be small compared with the source inhomogeneity scale) we can write $\mathbf{b} = \mathbf{b}_\omega e^{i\psi(\mathbf{r}) - i\omega t}$ and a similar for \mathbf{u} , which yields equations for the corresponding complex amplitudes:

$$\mathbf{b} = (i/\omega)[i(\mathbf{B}_0 \cdot \nabla\psi)\mathbf{u} - (\mathbf{u} \cdot \nabla)\mathbf{B}_0], \quad (2.102a)$$

$$\mathbf{u} = \frac{i\alpha_{FFF}}{4\pi\rho\omega} \mathbf{B}_0 \times \mathbf{b} - \frac{1}{4\pi\rho\omega} [(\mathbf{b} \cdot \mathbf{B}_0)\nabla\psi - (\mathbf{B}_0 \cdot \nabla\psi)\mathbf{b}]. \quad (2.102b)$$

Let us solve these equations to the first-order accuracy over the small parameter $\alpha_{FFF}/|\nabla\psi| \ll 1$. In the zeroth-order approximation we have

$$\mathbf{b} = -\frac{1}{\omega}(\mathbf{B}_0 \cdot \nabla\psi)\mathbf{u}, \quad \mathbf{u} = -\frac{1}{4\pi\rho\omega}(\mathbf{B}_0 \cdot \nabla\psi)\mathbf{b}, \quad (2.103)$$

which yields the eikonal

$$\nabla_{\parallel}\psi = \pm\omega/v_A, \quad v_A = B_0/\sqrt{4\pi\rho}. \quad (2.104)$$

It is easy to see that in the zeroth approximation these perturbations are identical to the purely alfvénic modes for which the conditions $\mathbf{b} \cdot \nabla\psi = 0$, $\mathbf{u} \cdot \nabla\psi = 0$, $\mathbf{b} \cdot \mathbf{B}_0 = 0$, and $\mathbf{u} \times \mathbf{b} = 0$ are satisfied.

Since we use the complex amplitudes, the bilinear terms like ab must be computed as $(1/2)\Re\langle ab^* \rangle$, where in addition to averaging over the period $T = 2\pi/\omega$ we also average over the random phases of Fourier harmonics:

$$\langle b_\mu b_\nu^* \rangle = (1/2)\langle b_\omega^2 \rangle (\delta_{\mu\nu} - e_\mu^\parallel e_\nu^\parallel). \quad (2.105)$$

In the zeroth over α_{FFF} approximation, the kinetic helicity parameter is zero: $\langle \mathbf{u} \cdot (\nabla \times \mathbf{u}^*) \rangle = 0$.

Now, taking into account the first order over $|\alpha_{FFF}/\nabla\psi|$ terms, Eq. (2.102b) yields

$$\mathbf{u} = -\frac{1}{4\pi\rho\omega}(\mathbf{B}_0 \cdot \nabla\psi)\mathbf{b} + \frac{1}{4\pi\rho\omega}[i\alpha_{FFF}\mathbf{B}_0 \times \mathbf{b} + (\mathbf{b} \cdot \mathbf{B}_0)\nabla\psi], \quad (2.106)$$

where $\mathbf{b} \cdot \mathbf{B}_0 \neq 0$ and

$$\begin{aligned} \nabla \times \mathbf{u} &= -\frac{i}{4\pi\rho\omega}(\mathbf{B}_0 \cdot \nabla\psi)(\nabla\psi \times \mathbf{b}) \\ &+ \frac{i}{4\pi\rho\omega}[-\nabla\psi \times (\mathbf{b} \cdot \nabla)\mathbf{B}_0 + \mathbf{b} \times (\mathbf{B}_0 \cdot \nabla)\nabla\psi + \mathbf{b} \times (\nabla\psi \cdot \nabla)\mathbf{B}_0]. \end{aligned} \quad (2.107)$$

These two expressions allow calculating the kinetic helicity density:

$$\frac{1}{2} \Re \langle \mathbf{u} \cdot (\nabla \times \mathbf{u}^*) \rangle = \frac{1}{4} \alpha_{FFF} v_A^2 \frac{\langle b_\omega^2 \rangle}{B_0^2}, \quad (2.108)$$

which is nonzero any longer; it is proportional to the magnetic field force-free parameter α_{FFF} and the wave intensity $\langle b_\omega^2 \rangle$.

2.7

$$B_x(y, z, t) = \left(B_{0y} \frac{\partial u_x}{\partial y} + B_{0z} \frac{\partial u_x}{\partial z} \right) t, \quad B_y = B_{0y}, \quad B_z = B_{0z}.$$

2.8

$$B_\alpha(r, \vartheta, t) = \sin \vartheta \left(r B_{0r}(r, \vartheta) \frac{\partial \Omega}{\partial r} + B_{0\vartheta} \frac{\partial \Omega}{\partial \vartheta} \right) t, \quad B_\vartheta = B_{0\vartheta}, \quad B_r = B_{0r}.$$

2.11 The field lines have a Archimedean spiral shape:

$$\begin{aligned} r &= \frac{u}{\Omega} (\alpha - \alpha_0), & \alpha_0 &= \text{const}, \\ \theta &= \arctan \frac{r_0 \Omega}{u} \approx 56^\circ; & B &\approx 4.5 \times 10^{-5} \text{ G}. \end{aligned}$$

Cosmic Electrodynamics

Electrodynamics and Magnetic Hydrodynamics of
Cosmic Plasmas

Fleishman, G.D.; Toptygin, I.N.

2013, XXII, 712 p., Hardcover

ISBN: 978-1-4614-5781-7